RESULTS

Expression of angiopoietins and the Tie-2 receptor in diabetic retinas: In situ hybridization was performed to analyze the expression of Ang-1, Ang-2, and Tie-2 in sections of eyes from STZ induced diabetic rats and then compare these patterns with those of non-diabetic control rats. An initial comparison between the body weight and plasma glucose levels of diabetic and control rats was also performed and is shown in Table 1. Diabetic rats had significantly lower body weights during the course of the experiment, 2 weeks to 6 months ($p<0.01$). Additionally, the plasma glucose levels of diabetic rats were significantly higher than those of the control rats ($p<0.01$). Ang-1 mRNA was expressed weakly in the ganglion cell layer (GCL) and the inner nuclear layer (INL; Figure 1). No remarkable difference was observed in Ang-1 expression between non-diabetic and STZ injected diabetic rats. Similarly, Ang-2 mRNA was also expressed weakly in the GCL and the INL (Figure 2). However, the expression level of Ang-2, although unchanged up to 3 months following STZ injection, increased at 6 months after STZ injection. Prominent Ang-2 expression was observed in the GCL of the diabetic rats at 6 months (Figure 2D). The Tie-2 receptor gene was also expressed in the GCL and the INL (Figure 3) but once again, no remarkable difference was observed between the expression of Tie-2 in non-diabetic and diabetic rats.

Increase of Ang-2 mRNA expression in the diabetic retina: To examine the relative expression levels of Ang mRNA during long term diabetes, semiquantitative RT-PCR experiments were performed using β-actin for normalization (Figure 4). Amplified PCR bands using both Ang-1 (372 bp) and Ang-2 primers (453 bp) were obtained from cDNA derived from the retinas of non-diabetic and diabetic rats six months after STZ injection. Ang-1 mRNA expression levels in diabetic retinas were equivalent to the non-diabetic control (Figure 4A, top). The mean±standard error of the mean expression in diabetic rats was 116±6% of that in non-diabetic controls (Figure 4B, top). In contrast to Ang-1, retinal expression of Ang-2 increased to 181±6% of controls 6 months after STZ injection (Figure 4A and Figure 4B, bottom).

Increase of Ang-2 protein expression in the diabetic retina: To elucidate expression levels of Ang-1, Ang-2 and Tie-2 protein in diabetic retinas, western blot analyses were performed. Consistent with the results of both in situ hybridization and RT-PCR analyses, Ang-2 protein expression was significantly ($p=0.039$) upregulated in retinas from diabetic rats compared to that from age matched non-diabetic control rats after 6 months. In contrast, both Ang-1 and Tie-2 protein levels were similar between diabetic and non-diabetic control rats at this time point (Ang-1, $p=0.1489$; Tie-2, $p=0.3865$; Figure 5A,B).

Increase of VEGF mRNA expression in the diabetic retina: We previously reported that VEGF, a central inducer of angiogenesis and whose expression is also reported to be increased in the diabetic retinas [25,26], can upregulate Ang-2 expression in endothelial cells [20]. To explore whether VEGF could be the inducer of Ang-2 expression in the diabetic retinas, we analyzed VEGF mRNA expression level in the diabetic retinas by real time PCR. VEGF mRNA expression was significantly ($p=0.0495$) upregulated in retinas from diabetic rats compared to that from age matched non-diabetic control rats after 6 months. The mean±standard error of the mean expression in diabetic rats was 233±44% of that in non-diabetic controls (Figure 5C).

Overexpression of Ang-2 is related to pericyte loss: To investigate changes in pericytes concurrent with Ang-2 overexpression, a double staining experiment using in situ

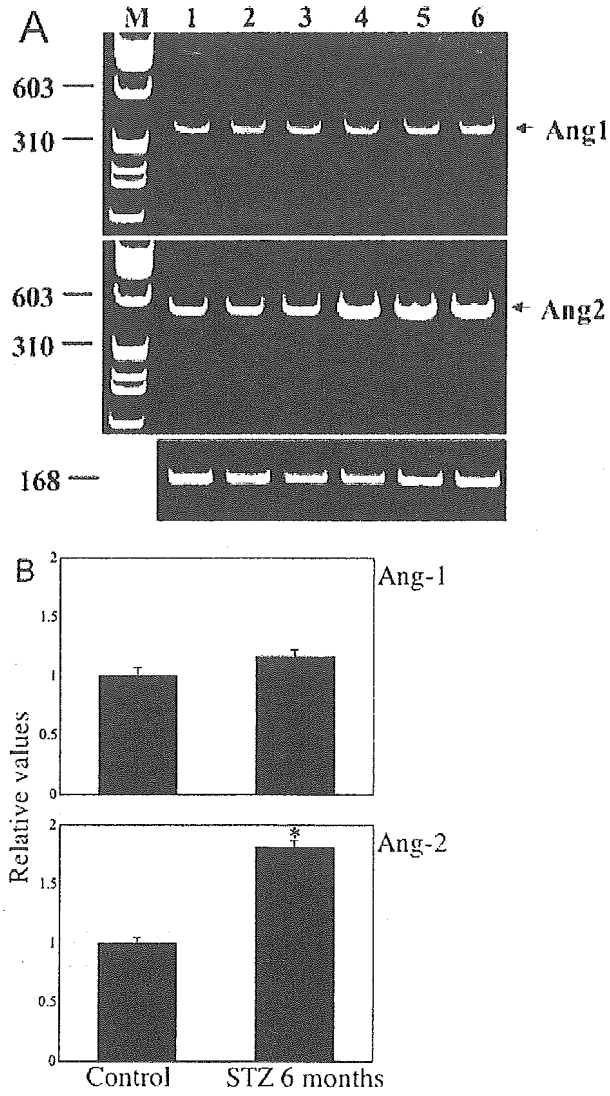

Figure 4. RT-PCR experiments to determine Ang-1 and Ang-2 gene expression in 6 months diabetic and control retinas. PCR was performed using (**A**, top) Ang-1 primers and (**A**, middle) Ang-2 primers after cDNA concentration was normalized to (**A**, bottom) β-actin gene expression. PCR products of expected lengths (Ang-1: 372 bp and Ang-2: 453 bp) were obtained (arrow). Lane 1-3: non-diabetic control rats; lane 4-6; diabetic rats; Lane M: X174/HaeIII marker. **B**: Relative intensities of PCR bands (top: Ang-1, bottom: Ang-2). In contrast to Ang-1, retinal expression of Ang-2 increased 6 months after STZ injection. An asterisk ("*") indicates $p<0.0005$ compared to control.

hybridization and immunohistochemistry was performed. Initially, retinas were stained by in situ hybridization using an Ang-2 probe and at 6 months following STZ injection, prominent Ang-2 expression was observed in the GCL. The same slides were used for immunohistochemical staining using an anti-αSMA antibody as a marker for periendothelial cells. In retinas of non-diabetic control rats, Ang-2 mRNA expression was observed only very weakly in the GCL and INL, while αSMA positive cells were observed in the GCL and the INL (Figure 6, left). In retinas of diabetic rats, Ang-2 mRNA expression was observed prominently in the GCL and INL, but αSMA positive pericytes decreased in both these regions compared to non-diabetic controls (Figure 6, right). Furthermore, this decrease of αSMA positive cells was especially prominent in areas alongside Ang-2 expressing cells.

DISCUSSION

Interaction between endothelial cells and pericytes has been shown to be a key regulatory mechanism for the functional properties of endothelial cells. The contact induced inhibitory effect of pericytes on the proangiogenic activity of endothelial cells is dependent, at least in part, on plasmin mediated activation of the latent form of TGF-β, which is produced by both pericytes and endothelial cells [27]. Based on the findings from Ang-1 knockout and Ang-2 transgenic mice, Ang-2 is suggested to play a role in suppressing such pericyte-endothelial cell interactions [28,29]. Indeed, Ang-2 expression is prominently upregulated in neovascular vessels where peri-endothelial cells are degenerative [30]. Therefore, we hypothesized that Ang-2 may be causally linked to pericyte loss in diabetic retinopathy. In the study described herein, we first demonstrated that Ang-2 is upregulated in the retina of diabetic rats whereas Ang-1 and Tie-2 are relatively stable. Ang-2 upregulation was observed in the GCL and the INL and with co-staining of SMA, we found that this upregulation correlated with depletion of peri-endothelial cells. These data suggest that an increase in Ang-2 might have possible effects on pericyte loss in diabetic retinas.

In adults, Ang-1 is constitutively expressed but regulation of this expression was demonstrated only during tumorigenesis [31,32] and in the ovulatory cycle [14,33]. The regulation of the Ang-1 gene in the retinas of diabetic animals has not been previously reported. In the present study, we have demonstrated using in situ hybridization that Ang-1 mRNA is expressed weakly in the GCL and the INL. The Tie-2 gene was also expressed in the GCL and the INL and it has been shown that in adult organs, constitutive expression of Ang-1 with concomitant phosphorylation of Tie-2 receptor tyrosine residues suggests that Tie-2 activity is important for the maintenance of a quiescent mature vasculature [34].

We also found no remarkable alterations in Ang-1 and Tie-2 expression between non-diabetic rats and STZ injected diabetic rats during the 6 months period that we performed our experiments. Ang-1 has been shown to inhibit diabetes induced leukocyte adhesion and subsequent endothelial damage [35]. Ang-1 is also reported to suppress diabetes induced

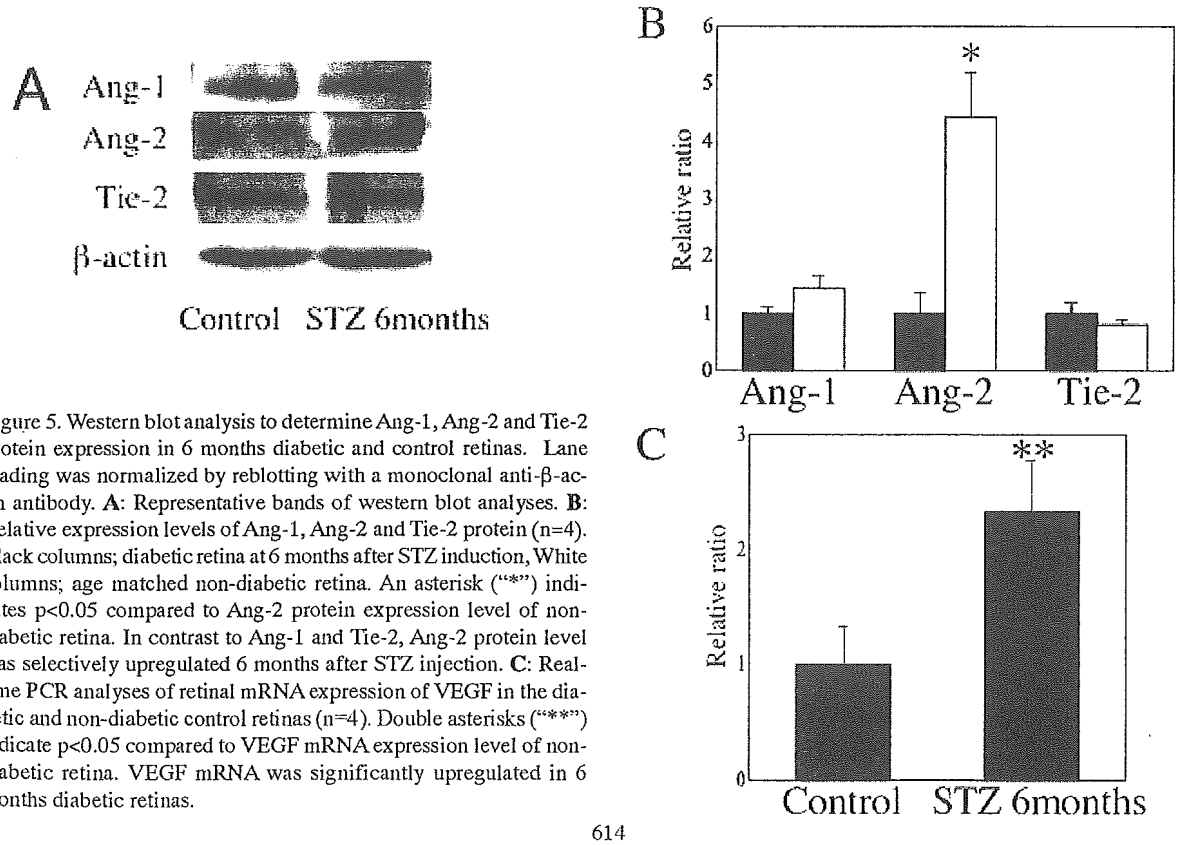

Figure 5. Western blot analysis to determine Ang-1, Ang-2 and Tie-2 protein expression in 6 months diabetic and control retinas. Lane loading was normalized by reblotting with a monoclonal anti-β-actin antibody. **A**: Representative bands of western blot analyses. **B**: Relative expression levels of Ang-1, Ang-2 and Tie-2 protein (n=4). Black columns; diabetic retina at 6 months after STZ induction, White columns; age matched non-diabetic retina. An asterisk ("*") indicates $p<0.05$ compared to Ang-2 protein expression level of non-diabetic retina. In contrast to Ang-1 and Tie-2, Ang-2 protein level was selectively upregulated 6 months after STZ injection. **C**: Real-time PCR analyses of retinal mRNA expression of VEGF in the diabetic and non-diabetic control retinas (n=4). Double asterisks ("**") indicate $p<0.05$ compared to VEGF mRNA expression level of non-diabetic retina. VEGF mRNA was significantly upregulated in 6 months diabetic retinas.

increases in retinal vasculature leakage [35]. These data suggest that it is not likely that alterations in expression of these genes are the primary mechanisms of diabetes induced pathologies. To know if Ang-1 is changed earlier, further time course experiments will be necessary.

Similar to Ang-1, Ang-2 mRNA was expressed only weakly in the GCL and the INL, the localization of which is consistent with the report of Hackett et al [29]. In their study, using the Ang-2 heterozygous mouse, Ang-2 expressed by neural cells is associated with the changes of retinal oxygen supplies and vascular remodeling in GCL and INL. In the present study, we have demonstrated for the first time that Ang-2 mRNA expression is upregulated in diabetic retinas. Following in situ hybridization experiments, Ang-2 expression was unchanged from 2 weeks to 3 months after STZ injection but was increased at 6 months. Prominent Ang-2 expression was observed in the GCL and the increase in the retinal expression levels of Ang-2 were confirmed by both RT-PCR and western blot analyses. The localization of Ang-2 suggests that Ang-2 might have effects on neural cells and indirect effects on vascular cells in the diabetic retinas [36]. Additionally, since TaqMan PCR would give a more detailed data than RT-PCR, further evaluation of expression levels of these molecules using TaqMan PCR are required in a future study.

At an early stage of tumorigenesis, Ang-2 has been shown to be induced in tumor microvessels, resulting in the disruption of the endothelial cell-pericyte interaction, endothelial apoptosis, and vessel regression [37,38]. In glioblastoma histology, Ang-2 has also been shown to be locally upregulated in the area of the disruption of endothelial and pericyte interaction [31]. In the present study, we also observed disruption of endothelial cell-pericyte interaction in the areas where Ang-2 is upregulated. These findings might suggest that selective Ang-2 increase might be a possible pathway for pericyte degeneration and loss or the neuronal retinal changes observed in diabetes. However, in our study, there is not sufficient data about the causal relationship between Ang-2 increase and retinal pericyte loss. Pericytes might be dying in spite of Ang-2 upregulation as well as because of it in the diabetic retinas.

Ang-2 has been reported to act differently in the absence and presence of VEGF. In the presence of VEGF, Ang-2 plays a proangiogenic role. By contrast, Ang-2 promotes endothelial cell death and vessel regression in the absence of VEGF [39,40]. Additionally, retinal VEGF mRNA was shown to be upregulated by experimental diabetes [25,26] and VEGF has been reported to upregulate Ang-2 expression in retinal endothelial cells [20]. Consistent with these reports, VEGF mRNA was significantly upregulated in 6 months diabetic retinas in the present study. These results suggest that VEGF in-

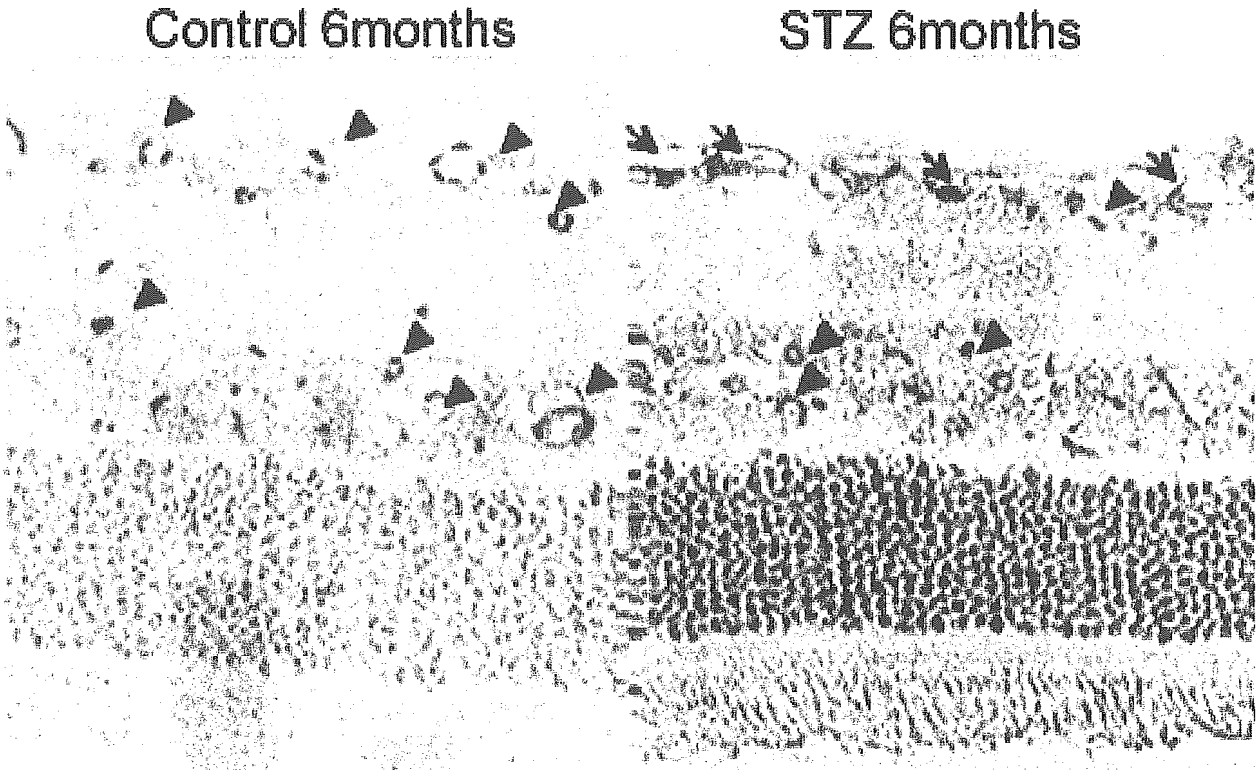

Figure 6. In situ hybridization analysis of Ang-2 expression followed by co-staining with anti-αSMA antibody. Control and 6 months diabetic animals were compared. Ang-2 mRNA expression were observed in the GCL and the INL (arrow head) in control animals and was increased in these layer by diabetes. αSMA positive cells were stained in the GCL and the INL (arrow). In diabetic rats, αSMA positive staining decreased compared to non-diabetic rats specifically in regions surrounding Ang-2 overexpressing cells.

duced upregulation of Ang-2 might stimulate pericyte loss and play proangiogenic roles in diabetic retinopathy. In contrast, recombinant Ang-1 had been reported to rescue retinal disorders induced by the absence of perivascular mural cells [41]. These studies suggest that the local treatment of recombinant Ang-1 might be a new therapeutic way to stabilize vessels by protecting the dropout of perivascular cells and that, in contrast, administration of recombinant Ang-2 in the presence of abundant VEGF might exacerbate diabetic retinopathy by promoting neovascularization. To fully delineate the causal relationship between Ang and pericyte loss in the diabetic retinas, further experiments such as administration of Ang-1 or Ang 2 and Ang over expressing transgenic animals will be necessary in the future study.

ACKNOWLEDGEMENTS

This work was supported by grants in aid for scientific research from the Ministry of Education, Science, and Culture and the Ministry of Health and Welfare of the Japanese Government (70283596).

REFERENCES

1. Kador PF, Akagi Y, Terubayashi H, Wyman M, Kinoshita JH. Prevention of pericyte ghost formation in retinal capillaries of galactose-fed dogs by aldose reductase inhibitors. Arch Ophthalmol 1988; 106:1099-102.
2. Robison WG Jr, McCaleb ML, Feld LG, Michaelis OE 4th, Laver N, Mercandetti M, Robinson WG Jr. Degenerated intramural pericytes ('ghost cells') in the retinal capillaries of diabetic rats. Curr Eye Res 1991; 10:339-50. Erratum in: Curr Eye Res 1991; 10:893.
3. Li W, Yanoff M, Liu X, Ye X. Retinal capillary pericyte apoptosis in early human diabetic retinopathy. Chin Med J (Engl) 1997; 110:659-63.
4. Hammes HP, Lin J, Renner O, Shani M, Lundqvist A, Betsholtz C, Brownlee M, Deutsch U. Pericytes and the pathogenesis of diabetic retinopathy. Diabetes 2002; 51:3107-12.
5. Amano S, Yamagishi S, Kato N, Inagaki Y, Okamoto T, Makino M, Taniko K, Hirooka H, Jomori T, Takeuchi M. Sorbitol dehydrogenase overexpression potentiates glucose toxicity to cultured retinal pericytes. Biochem Biophys Res Commun 2002; 299:183-8.
6. de la Rubia G, Oliver FJ, Inoguchi T, King GL. Induction of resistance to endothelin-1's biochemical actions by elevated glucose levels in retinal pericytes. Diabetes 1992; 41:1533-9.
7. Park JY, Takahara N, Gabriele A, Chou E, Naruse K, Suzuma K, Yamauchi T, Ha SW, Meier M, Rhodes CJ, King GL. Induction of endothelin-1 expression by glucose: an effect of protein kinase C activation. Diabetes 2000; 49:1239-48.
8. Beltramo E, Pomero F, Allione A, D'Alu F, Ponte E, Porta M. Pericyte adhesion is impaired on extracellular matrix produced by endothelial cells in high hexose concentrations. Diabetologia 2002; 45:416-9.
9. Yamagishi S, Amano S, Inagaki Y, Okamoto T, Koga K, Sasaki N, Yamamoto H, Takeuchi M, Makita Z. Advanced glycation end products-induced apoptosis and overexpression of vascular endothelial growth factor in bovine retinal pericytes. Biochem Biophys Res Commun 2002; 290:973-8.
10. Yamagishi S, Inagaki Y, Amano S, Okamoto T, Takeuchi M, Makita Z. Pigment epithelium-derived factor protects cultured retinal pericytes from advanced glycation end product-induced injury through its antioxidative properties. Biochem Biophys Res Commun 2002; 296:877-82.
11. Shojaee N, Patton WF, Hechtman HB, Shepro D. Myosin translocation in retinal pericytes during free-radical induced apoptosis. J Cell Biochem 1999; 75:118-29.
12. Romeo G, Liu WH, Asnaghi V, Kern TS, Lorenzi M. Activation of nuclear factor-kappaB induced by diabetes and high glucose regulates a proapoptotic program in retinal pericytes. Diabetes 2002; 51:2241-8.
13. Joussen AM, Poulaki V, Mitsiades N, Cai WY, Suzuma I, Pak J, Ju ST, Rook SL, Esser P, Mitsiades CS, Kirchhof B, Adamis AP, Aiello LP. Suppression of Fas-FasL-induced endothelial cell apoptosis prevents diabetic blood-retinal barrier breakdown in a model of streptozotocin-induced diabetes. FASEB J 2003; 17:76-8.
14. Maisonpierre PC, Suri C, Jones PF, Bartunkova S, Wiegand SJ, Radziejewski C, Compton D, McClain J, Aldrich TH, Papadopoulos N, Daly TJ, Davis S, Sato TN, Yancopoulos GD. Angiopoietin-2, a natural antagonist for Tie2 that disrupts in vivo angiogenesis. Science 1997; 277:55-60.
15. Davis S, Aldrich TH, Jones PF, Acheson A, Compton DL, Jain V, Ryan TE, Bruno J, Radziejewski C, Maisonpierre PC, Yancopoulos GD. Isolation of angiopoietin-1, a ligand for the TIE2 receptor, by secretion-trap expression cloning. Cell 1996; 87:1161-9.
16. Sato TN, Qin Y, Kozak CA, Audus KL. Tie-1 and tie-2 define another class of putative receptor tyrosine kinase genes expressed in early embryonic vascular system. Proc Natl Acad Sci U S A 1993; 90:9355-8. Erratum in: Proc Natl Acad Sci U S A 1993; 90:12056.
17. Sato TN, Tozawa Y, Deutsch U, Wolburg-Buchholz K, Fujiwara Y, Gendron-Maguire M, Gridley T, Wolburg H, Risau W, Qin Y. Distinct roles of the receptor tyrosine kinases Tie-1 and Tie-2 in blood vessel formation. Nature 1995; 376:70-4.
18. Dumont DJ, Gradwohl G, Fong GH, Puri MC, Gertsenstein M, Auerbach A, Breitman ML. Dominant-negative and targeted null mutations in the endothelial receptor tyrosine kinase, tek, reveal a critical role in vasculogenesis of the embryo. Genes Dev 1994; 8:1897-909.
19. Vikkula M, Boon LM, Carraway KL 3rd, Calvert JT, Diamonti AJ, Goumnerov B, Pasyk KA, Marchuk DA, Warman ML, Cantley LC, Mulliken JB, Olsen BR. Vascular dysmorphogenesis caused by an activating mutation in the receptor tyrosine kinase TIE2. Cell 1996; 87:1181-90.
20. Oh H, Takagi H, Suzuma K, Otani A, Matsumura M, Honda Y. Hypoxia and vascular endothelial growth factor selectively up-regulate angiopoietin-2 in bovine microvascular endothelial cells. J Biol Chem 1999; 274:15732-9.
21. Otani A, Takagi H, Suzuma K, Honda Y. Angiotensin II potentiates vascular endothelial growth factor-induced angiogenic activity in retinal microcapillary endothelial cells. Circ Res 1998; 82:619-28.
22. Mandriota SJ, Pepper MS. Regulation of angiopoietin-2 mRNA levels in bovine microvascular endothelial cells by cytokines and hypoxia. Circ Res 1998; 83:852-9.
23. Nudel U, Zakut R, Shani M, Neuman S, Levy Z, Yaffe D. The nucleotide sequence of the rat cytoplasmic beta-actin gene. Nucleic Acids Res 1983; 11:1759-71.
24. Philp NJ, Ochrietor JD, Rudoy C, Muramatsu T, Linser PJ. Loss of MCT1, MCT3, and MCT4 expression in the retinal pigment epithelium and neural retina of the 5A11/basigin-null mouse. Invest Ophthalmol Vis Sci 2003; 44:1305-11.

25. Punglia RS, Lu M, Hsu J, Kuroki M, Tolentino MJ, Keough K, Levy AP, Levy NS, Goldberg MA, D'Amato RJ, Adamis AP. Regulation of vascular endothelial growth factor expression by insulin-like growth factor I. Diabetes 1997; 46:1619-26.
26. Moravski CJ, Skinner SL, Stubbs AJ, Sarlos S, Kelly DJ, Cooper ME, Gilbert RE, Wilkinson-Berka JL. The renin-angiotensin system influences ocular endothelial cell proliferation in diabetes: transgenic and interventional studies. Am J Pathol 2003; 162:151-60.
27. Sato Y, Rifkin DB. Inhibition of endothelial cell movement by pericytes and smooth muscle cells: activation of a latent transforming growth factor-beta 1-like molecule by plasmin during co-culture. J Cell Biol 1989; 109:309-15.
28. Suri C, Jones PF, Patan S, Bartunkova S, Maisonpierre PC, Davis S, Sato TN, Yancopoulos GD. Requisite role of angiopoietin-1, a ligand for the TIE2 receptor, during embryonic angiogenesis. Cell 1996; 87:1171-80.
29. Hackett SF, Ozaki H, Strauss RW, Wahlin K, Suri C, Maisonpierre P, Yancopoulos G, Campochiaro PA. Angiopoietin 2 expression in the retina: upregulation during physiologic and pathologic neovascularization. J Cell Physiol 2000; 184:275-84.
30. Liu W, Reinmuth N, Stoeltzing O, Parikh AA, Fan F, Ahmad SA, Jung YD, Ellis LM. Antiangiogenic therapy targeting factors that enhance endothelial cell survival. Semin Oncol 2002; 29:96-103.
31. Stratmann A, Risau W, Plate KH. Cell type-specific expression of angiopoietin-1 and angiopoietin-2 suggests a role in glioblastoma angiogenesis. Am J Pathol 1998; 153:1459-66.
32. Zagzag D, Hooper A, Friedlander DR, Chan W, Holash J, Wiegand SJ, Yancopoulos GD, Grumet M. In situ expression of angiopoietins in astrocytomas identifies angiopoietin-2 as an early marker of tumor angiogenesis. Exp Neurol 1999; 159:391-400.
33. Goede V, Schmidt T, Kimmina S, Kozian D, Augustin HG. Analysis of blood vessel maturation processes during cyclic ovarian angiogenesis. Lab Invest 1998; 78:1385-94.
34. Wong AL, Haroon ZA, Werner S, Dewhirst MW, Greenberg CS, Peters KG. Tie2 expression and phosphorylation in angiogenic and quiescent adult tissues. Circ Res 1997; 81:567-74.
35. Joussen AM, Poulaki V, Tsujikawa A, Qin W, Qaum T, Xu Q, Moromizato Y, Bursell SE, Wiegand SJ, Rudge J, Ioffe E, Yancopoulos GD, Adamis AP. Suppression of diabetic retinopathy with angiopoietin-1. Am J Pathol 2002; 160:1683-93.
36. Hackett SF, Wiegand S, Yancopoulos G, Campochiaro PA. Angiopoietin-2 plays an important role in retinal angiogenesis. J Cell Physiol 2002; 192:182-7.
37. Holash J, Wiegand SJ, Yancopoulos GD. New model of tumor angiogenesis: dynamic balance between vessel regression and growth mediated by angiopoietins and VEGF. Oncogene 1999; 18:5356-62.
38. Holash J, Maisonpierre PC, Compton D, Boland P, Alexander CR, Zagzag D, Yancopoulos GD, Wiegand SJ. Vessel cooption, regression, and growth in tumors mediated by angiopoietins and VEGF. Science 1999; 284:1994-8.
39. Asahara T, Chen D, Takahashi T, Fujikawa K, Kearney M, Magner M, Yancopoulos GD, Isner JM. Tie2 receptor ligands, angiopoietin-1 and angiopoietin-2, modulate VEGF-induced postnatal neovascularization. Circ Res 1998; 83:233-40.
40. Lobov IB, Brooks PC, Lang RA. Angiopoietin-2 displays VEGF-dependent modulation of capillary structure and endothelial cell survival in vivo. Proc Natl Acad Sci U S A 2002; 99:11205-10.
41. Uemura A, Ogawa M, Hirashima M, Fujiwara T, Koyama S, Takagi H, Honda Y, Wiegand SJ, Yancopoulos GD, Nishikawa S. Recombinant angiopoietin-1 restores higher-order architecture of growing blood vessels in mice in the absence of mural cells. J Clin Invest 2002; 110:1619-28.

The print version of this article was created on 26 Aug 2004. This reflects all typographical corrections and errata to the article through that date. Details of any changes may be found in the online version of the article.

ELSEVIER

Journal of the Neurological Sciences 225 (2004) 135–141

Journal of the Neurological Sciences

www.elsevier.com/locate/jns

Prediction of psychiatric response to donepezil in patients with mild to moderate Alzheimer's disease

Makoto Tanaka[a,*], Chihiro Namiki[b], Dinh Ha Duy Thuy[b], Hidefumi Yoshida[b], Keiichi Kawasaki[b], Kazuo Hashikawa[b], Hidenao Fukuyama[b], Toru Kita[c]

[a]*Department of Social Service, Kyoto University Hospital, 54 Shogoin-Kawahara-cho, Sakyo-ku, Kyoto 606-8507, Japan*
[b]*Human Brain Research Center, Graduate School of Medicine, Kyoto University, Kyoto, Japan*
[c]*Department of Cardiovascular Medicine, Graduate School of Medicine, Kyoto University, Kyoto, Japan*

Received 17 March 2004; received in revised form 13 July 2004; accepted 15 July 2004
Available online 25 August 2004

Abstract

Donepezil is a selective acetylcholinesterase inhibitor approved for the symptomatic treatment of mild to moderate Alzheimer's disease (AD). Since behavioral symptoms severely affect quality of life for AD patients and their caregivers, predicting behavioral responses to donepezil will be useful in managing patients with AD. In this study, we analyzed 70 consecutive cases with mild to moderate AD. Caregivers were interviewed with the Neuropsychiatric Inventory for behavioral assessment and 4-point improvement at week 12 was accepted as a treatment response. Twenty-one (30.0%) patients showed a behavioral response, while 42 (60.0%) showed no behavioral change and 7 (10.0%) worsened. Dysphoria, anxiety and apathy significantly improved after treatment among the responder group. The baseline profile including age, sex, Mini-Mental State Examination (MMSE), the Alzheimer's Disease Assessment Scale (ADAS-cog) and the Geriatric Depression Scale did not differ significantly among the three groups. Statistical Parametric Mapping analysis of single photon emission computed tomography (SPECT) images at baseline showed that cerebral blood flow in the premotor and parietotemporal cortices was significantly higher in the responder group than in the worse group. The present study suggested usefulness of SPECT imaging in the prediction of behavioral response to donepezil among AD patients even with similar psychiatric symptoms and cognitive functions.

Keywords: Alzheimer's disease; Donepezil; SPECT; Psychiatric symptom

1. Introduction

Donepezil hydrochloride, a selective acetylcholinesterase inhibitor, has received widespread approval for the symptomatic treatment of Alzheimer's disease (AD). A series of clinical trials suggested that donepezil improved behavioral abnormalities as well as cognitive and global function in patients with mild to moderate AD [1–5]. Significant treatment benefit was already observed as early as 12 weeks on the Mini-Mental State Examination (MMSE), the cognitive portion of the Alzheimer's Disease Assessment Scale (ADAS-cog) and the Clinician's Interview Based Assessment of Change-Plus (CIBIC plus) [2–5]. However, not all patients respond to donepezil; some patients show progressive cognitive decline in spite of cholinergic therapy. Psychotropic effects of donepezil are also variable from marked to no improvement.

Recently, functional neuroimaging studies have shown that regional cerebral blood flow was better preserved in AD patients receiving donepezil [6]. Moreover, Nobili et al. [7] compared donepezil-effective and noneffective groups and found that no significant perfusion reduction was observed between the baseline and repeated single photon emission computed tomography (SPECT) data in the donepezil-effective group over a 1-year period. However, these studies did not identify any significant baseline differences between

* Corresponding author.
E-mail address: makoto@kuhp.kyoto-u.ac.jp (M. Tanaka).

0022-510X/$ - see front matter © 2004 Elsevier B.V. All rights reserved.
doi:10.1016/j.jns.2004.07.009

responders and nonresponders, which would be useful in predicting responses to donepezil. Hanyu et al. [8] demonstrated that regional cerebral blood flow (rCBF) in the lateral and medial frontal lobes at baseline may predict cognitive response to donepezil, although these patients were only evaluated by Mini-Mental State Examination (MMSE).

Data are even more limited regarding the prediction of behavioral response to donepezil. Mega et al. [9] characterized profiles of patients who behaviorally responded to donepezil, showing that responders had worse psychotic symptoms at baseline. Moreover, they examined a subset of these patients who had SPECT imaging available for analysis and demonstrated a lower blood flow in orbito- and dorsolateral frontal cortex at baseline in AD patients with a good behavioral response to donepezil [10]. However, it was not clear whether the baseline difference in regional cerebral blood flow was a predictor of behavioral response to donepezil or merely reflected brain regions responsible for psychotic symptoms, because responders had significantly more pretreatment behavioral abnormalities than nonresponders in their retrospective study [10].

Behavioral abnormalities have a major impact on quality of life for AD patients and caregiver burden [11–15]. For example, apathetic patients have increased reliance on caregivers to initiate and oversee activities, require more support and place higher levels of burden on caregivers [14]. Notably, the overall distribution of caregiver ratings on social behavior including patient interaction with others, initiation and engagement in pleasurable activities and participation in conversation was significantly better for donepezil-treated patients and their caregivers reported lower levels of stress [15]. Thus, predicting behavioral responses to donepezil will be important in the management of patients with AD. In this study, we focused on behavioral effects of donepezil, using the response on the Neuropsychiatric Inventory (NPI) as the outcome measure and analyzed 70 consecutive patients with mild to moderate AD to address whether SPECT data at initial evaluation could predict behavioral responses to donepezil.

2. Material and methods

2.1. Subjects and clinical assessment

Patient recruitment for this study began in October 2000 and terminated in March 2003. All study participants presented for dementia evaluation to the memory clinic of the Department of Geriatric Medicine, Kyoto University Hospital. They were invited to participate in the study if they met National Institute of Neurological and Communicative Disorders and Stroke–Alzheimer's Disease and Related Disorders Association criteria for probable AD [16], had mild to moderate AD defined by a MMSE score of $\geq$16, were free of psychiatric or neurological disease other than dementia, had no major medical illnesses that were not clinically stable and were taking no medications that could affect psychiatric symptoms or cognitive functions.

Patients were evaluated by complete medical history taking, physical examination and neuropsychological test batteries including MMSE and ADAS-cog. All patients underwent magnetic resonance imaging or computed tomography, and SPECT. Patients and their caregivers were informed of the aim of the neuropsychological tests and neuroimaging examinations and gave their consent. Caregivers were interviewed with the Neuropsychiatric Inventory (NPI) [17] for behavioral assessment and the Barthel Index [18] and Lawton instrumental activities of daily living (ADL) scale [19] for functional evaluation.

All patients and caregivers agreed to treatment with donepezil. Patients received 3 mg/day donepezil for the first 2 weeks and 5 mg/day thereafter. (Five milligrams are the maximum dose permitted in Japan.) Because previous double-blind placebo-controlled studies with donepezil have shown a significant effect after 8 weeks, [5] we evaluated the patients at baseline and week 12. According to Mega et al. [9,10], a 4-point improvement on the NPI was accepted as evidence of a treatment response and a 4-point decrement as evidence of treatment failure. After 12 weeks of therapy, patients were classified into three groups: (1) Group 1 (improved; $\geq$4 point reduction in total NPI score), (2) Group 2 (unchanged; $\leq$3 point decrease or increase in total NPI score), (3) Group 3 (worse; $\geq$4 point increase in total NPI score).

2.2. SPECT image acquisition and analysis

Subjects were injected with 222 MBq of ^{123}I-isopropyliodoamphetamine (IMP) with eyes open and ears unplugged in a quiet room. Ten minutes after injection, scanning was performed parallel to the canthomeatal line using a three-head gamma camera PRISM 3000 XP (Picker, Cleveland, OH) equipped with ultrahigh-resolution fanbeam collimators. The scanned data were prefiltered on a workstation (Odyssey, Picker) using a Butterworth filter (order 4 and a cut off at 0.26 cycles/pixel) and were reconstructed with a Ramp filter at 128×128 pixels with 40 slices (1.7×1.7×3.4 mm in actual size of voxel). A postreconstruction attenuation correction was applied with an attenuation coefficient of 0.09/cm.

The SPECT data were analyzed by Statistical Parametric Mapping 99 (SPM99) (Wellcome Department of Neurology, Institute of Neurology, University College London, UK) with MATLAB (Mathworks, Sherborn, MA, USA) on a Sun Ultra-2 workstation (Sun Microsystems, Mountain View, CA, USA). The SPECT images were normalized to the standard brain atlas provided in the SPM99 template for SPECT. Statistical significance was set at 0.001.

Table 1
Subject demographics

	Group 1	Group 2	Group 3
N	21 (30.0%)	42 (60.0%)	7 (10.0%)
Age	76.8±6.9	74.1±9.2	73.6±6.5
Sex (M/F)	9/12	16/26	3/4
Education (years)	11.7±3.2	10.6±3.0	10.7±4.5
MMSE	21.2±4.2	21.6±4.2	23.3±2.6
ADAS-cog	17.5±8.1	14.4±6.4	16.6±4.8
Barthel	95.7±9.7	97.1±6.4	95.7±4.5
Lawton	4.1±2.4	4.4±1.9	4.8±1.8
GDS-15	5.1±2.7	3.8±2.5	5.3±3.1
NPI	10.8±6.4*	4.9±4.2*	7.7±5.7

Values are expressed as means±S.D. Mini-Mental State Examination (MMSE). Alzheimer's Disease Assessment Scale-cognitive subscales (ADAS-cog). Barthel Index (Barthel). Lawton instrumental activities of daily living scale (Lawton). The 15-item Geriatric Depression Scale (GDS-15). Neuropsychiatiric Inventory (NPI).
Demographic characteristics of subjects in Group 1 (improved), Group 2 (unchanged) and Group 3 (worse).
* Significantly different by Fischer's PLSD test.

2.3. Statistics

Two-tailed unpaired Student's *t*-test was applied to analyze data between two groups and one-factorial ANOVA followed by Fischer's PLSD test was used to compare data between more than three groups.

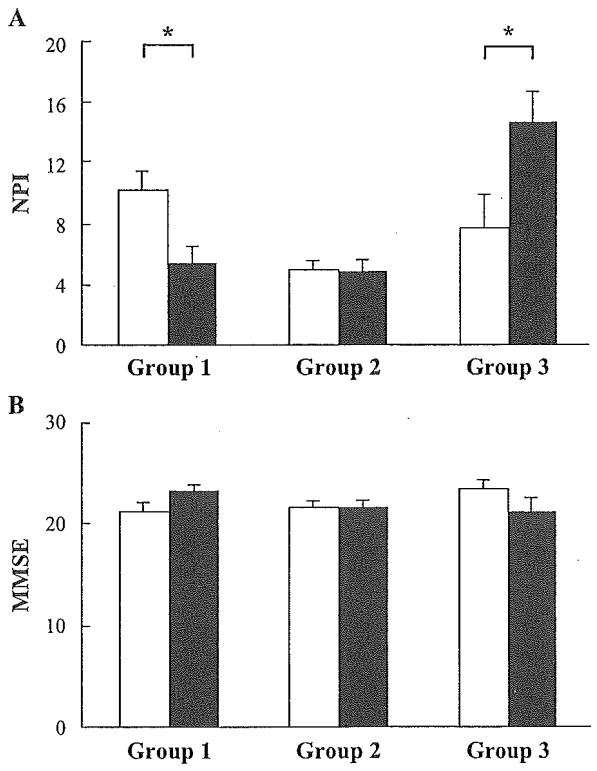

Fig. 1. (A) Mean total NPI scores at baseline (open bars) and at week 12 (closed bars). (B) Mean MMSE scores at baseline (open bars) and at week 12 (closed bars). The values are mean with standard error. *$p<0.01$.

3. Results

3.1. Subject demographics

Of the 74 patients initially recruited, two patients were lost during follow-up and two patients did not tolerate donepezil because of liver dysfunction and drug eruption, respectively. Therefore, the study group consisted of 70 consecutive outpatients who met the study criteria, were followed up for more than 12 weeks and tolerated 5 mg/day donepezil. Table 1 shows demographic characteristics of the groups based on their behavioral response to donepezil. Psychiatric symptoms improved in 21 patients (30.0%), while 42 (60.0%) showed no behavioral change and 7 (10.0%) worsened in spite of donepezil treatment. There were no significant differences at baseline in age, sex, education, cognitive functions measured by MMSE and ADAS-cog, basic and instrumental ADL and depression scale score among the three groups (Table 1). Total NPI scores at baseline were significantly higher in Group 1 than in Group 2, but there were no significant differences between Groups 1 and 3 (Table 1). There were no significant differences in frequency and severity of behav-

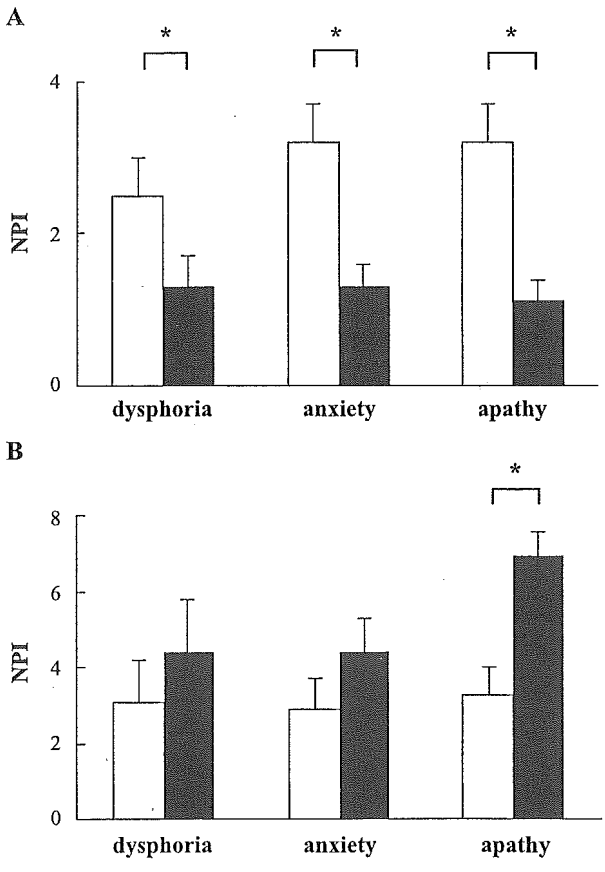

Fig. 2. (A) Mean NPI subscale scores at baseline (open bars) and at week 12 (closed bars) in Group 1. (B) Mean NPI subscale scores at baseline (open bars) and at week 12 (closed bars) in Group 3. The values are mean with standard error. *$p<0.01$.

ioral abnormalities across any NPI domains between Groups 1 and 3 (not shown).

Total NPI scores significantly decreased in Group 1 and increased in Group 3, while MMSE scores did not change within any group (Fig. 1). In Group 1, dysphoria, anxiety and apathy improved significantly after donepezil therapy (Fig. 2). In contrast, apathy significantly worsened in Group 3 in spite of donepezil treatment (Fig. 2).

3.2. SPECT image analysis

There were no significant differences at baseline in any profiles including cognitive functions and behavioral abnormalities between Groups 1 and 3. Can baseline SPECT data predict behavioral effects of donepezil? First, we visually inspected average SPECT images (Fig. 3). Average regional cerebral blood flow (rCBF) was decreased in the parietal, temporal and medial temporal lobes in all the three groups, indicating that all groups of patients had SPECT images typically suggestive of AD (Fig. 3). The rCBF in the frontal cortex was well preserved in Group 1 and the rCBF in the parietotemporal lobes was markedly reduced in Group 3 (Fig. 3).

We next compared SPECT images between groups using SPM analysis. Blood flow in the premotor cortex was better preserved in Group 1 than in Group 2 (Fig. 4). Moreover, the parietotemporal cortices were significantly hypoperfused in Group 3 as compared with Group 2 (Fig. 5). When Groups 1 and 3 were compared, rCBF was better preserved in the premotor, parietal and temporal cortices in Group 1 (Fig. 6).

We finally analyzed correlations between rCBF and specific NPI domains at baseline to see whether specific psychiatric symptoms affected rCBF. However, in our study population, there were no significant correlations between rCBF and any specific domains of the NPI.

4. Discussion

The major limitation of this study was a lack of a control group who received a placebo. One could argue that behavioral changes may have occurred spontaneously. However, the use of placebo controls was not ethically acceptable, because several clinical trials had demonstrated that donepezil improved cognitive and global functions in patients with AD [1–5]. Thus, we took a strategy of treating all the patients with donepezil and dividing them into the three groups. Another limitation was the small number of patients in Group 3. It is possible that some of the negative conclusions may simply reflect the low power derivable from the small sample. A strength of the study was the large overall number of patients included and the consecutive recruitment strategy.

In our cohort, Group 2 had fewer behavioral abnormalities both at baseline and week 12. This result was consistent with previous reports [9,10] and it can be assumed that this group represented AD patients with few

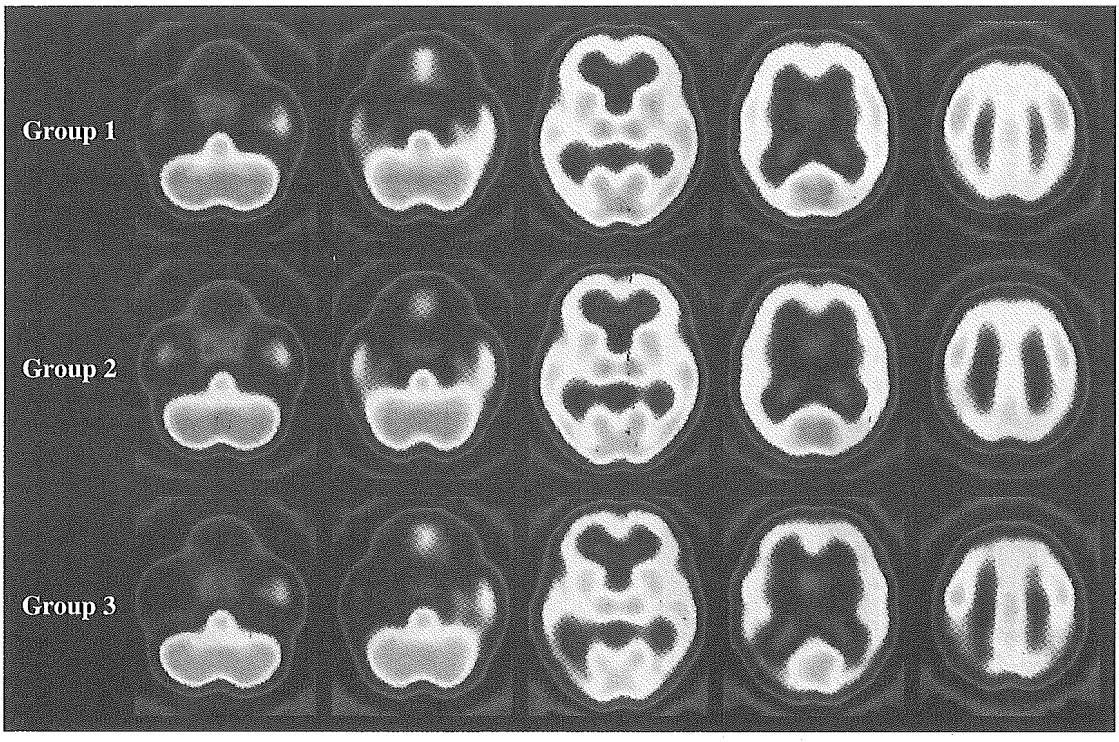

Fig. 3. Average SPECT images of Groups 1, 2 and 3.

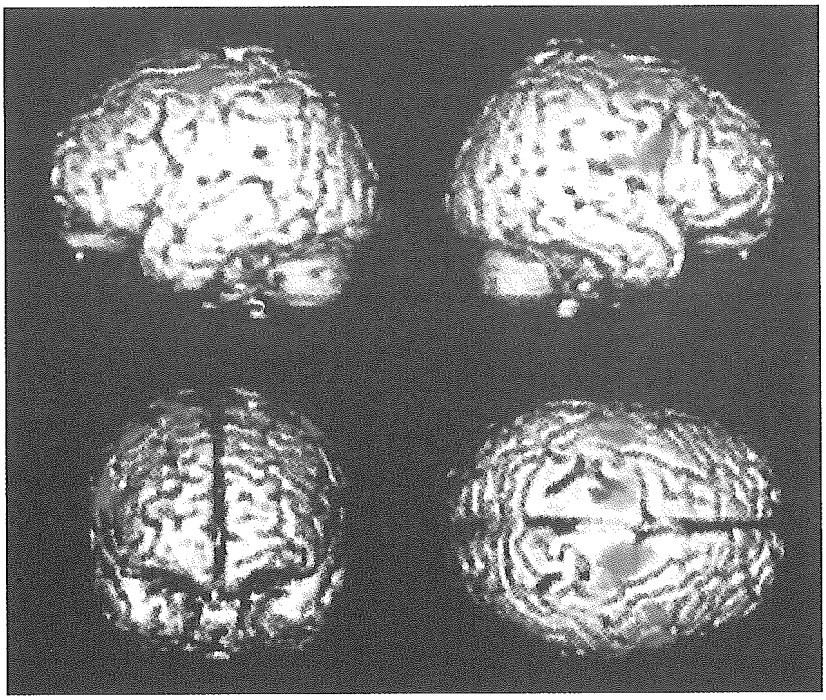

Fig. 4. Statistical parametric map overlaid on a surface-rendered standard anatomical image. The map reflects regions with significantly higher blood flow in Group 1 than in Group 2. Peak differences were found in the right medial frontal gyrus (Brodmann 6, x, y, z: 18, −8, 52; z score=−4.28), the left medial frontal gyrus (Brodmann 6, x, y, z: −14, −12, 56; z score=−3.70) and the left superior frontal gyrus (Brodmann 6, x, y, z: −50, −8, 64; z score=−3.43).

psychiatric symptoms. Groups 1 and 3 had more severe psychiatric symptoms than Group 2. Although there were no significant differences in both cognitive functions and psychiatric symptoms between Groups 1 and 3, each group showed striking differences in SPECT images, indicating that the differences in rCBF between Groups 1 and 3 were

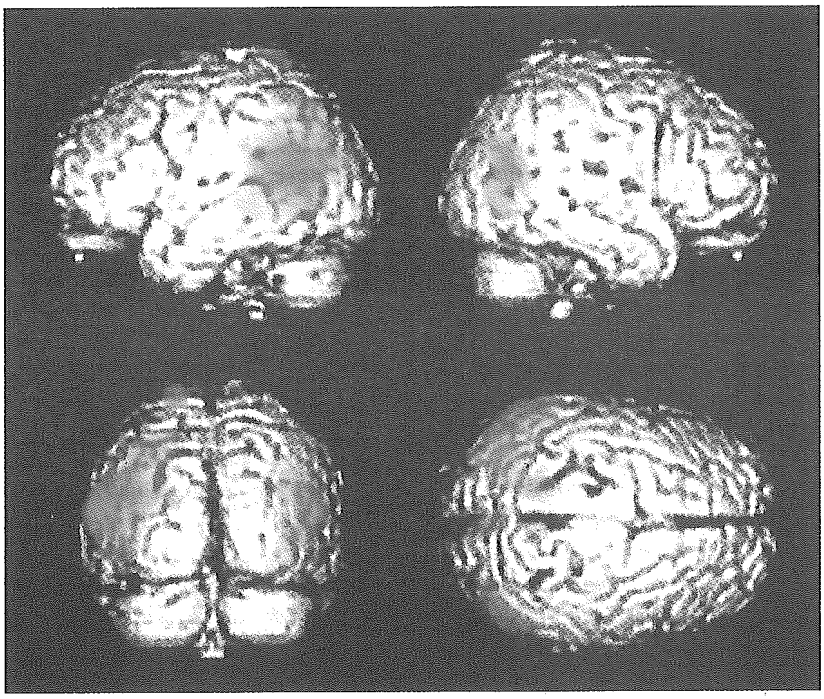

Fig. 5. Statistical parametric map overlaid on a surface-rendered standard anatomical image. The map reflects regions with significantly lower blood flow in Group 3 than in Group 2. Peak differences were found in the left inferior parietal lobule (Brodmann 39, x, y, z: −50, −54, 18; z score=−4.45), the left superior temporal gyrus (Brodmann 22, x, y, z: −42, −64, 0; z score=−3.81), the left middle temporal gyrus (Brodmann 39, x, y, z: −40, −66, 24; z score=−3.80), the left superior parietal lobule (Brodmann 7, x, y, z: −18, −46, 78; z score=−3.63) and the right middle temporal gyrus (Brodmann 39, x, y, z: 52, −64, 16; z score=−3.43).

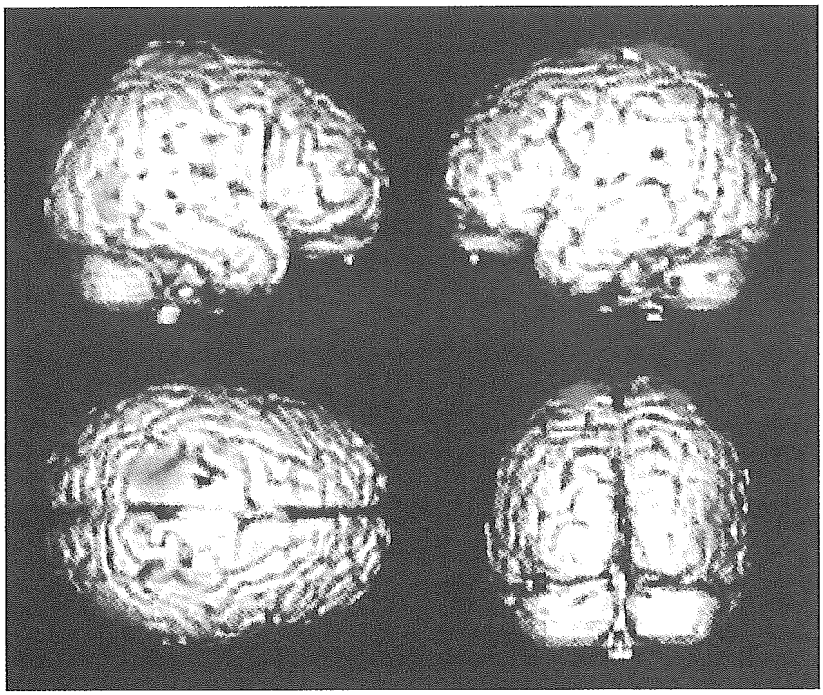

Fig. 6. Statistical parametric map overlaid on a surface-rendered standard anatomical image. The map reflects regions with significantly higher blood flow in Group 1 than in Group 3. Peak differences were found in the left superior parietal lobule (Brodmann 7, x, y, z: −18, −44, 78; z score=−4.48), the left superior frontal gyrus (Brodmann 6, x, y, z: −36, −10, 74; z score=−3.32) and the right superior parietal lobule (Brodmann 7, x, y, z: 32, −38, 74; z score=−3.10).

unlikely to reflect differences in baseline psychiatric symptoms or cognitive functions. The present study demonstrated that patterns of rCBF deficit were heterogeneous among AD patients and that the utility of SPECT and behavioral responses deserves more comprehensive investigation.

It may be too simplistic to relate blood flow patterns to global behavioral changes, since the NPI includes several different items such as apathy, irritability and aberrant movement. However, psychiatric symptoms significantly worse in Groups 1 and 3 were only dysphoria, anxiety and apathy. Moreover, out of the 10 items of the NPI, improvement in Group 1 was observed only in these three psychiatric symptoms, while these symptoms remained unimproved in Group 3. Therefore, it may be better to conclude that the difference in SPECT patterns between Groups 1 and 3 may be useful in predicting improvement of dysphoria, anxiety and apathy in AD patients treated with donepezil.

Donepezil may be effective if neurons are not functioning properly because of cholinergic depletion [20]. However, once neuronal loss occurs, effects of cholinergic therapy may not be expected. Severe hypoperfusion in the parietotemporal cortices in Group 3 suggested substantial neuronal loss in these regions. Functional brain mapping has demonstrated activation of the parietal and/or temporal cortices in abstract thinking, [21] categorization, [22] social judgment [23] and decision making [24]. Deficits in these cognitive areas may be related to worsening of psychiatric symptoms.

It has been suggested that the premotor cortex may play an important role in the working memory system [25–31]. Neuroimaging studies have shown that the premotor area was activated during tasks requiring verbal short-term storage [25,27–29,31], spatial memory [26,29,30] and executive processes such as attention control [32,33]. Moreover, the dorsal premotor cortex was activated in the conversion of working memory to motor sequence, which is required for serial movements and complex behaviors [34]. The preserved rCBF in the premotor cortex in Group 1 suggested that the better behavioral responses in this group may be associated with preservation of the working memory system.

Mega et al. demonstrated orbital and dorsolateral frontal perfusion defect in patients who behaviorally responded to donepezil. However, in their study, responders had much more severe psychiatric symptoms at baseline than non-responders [10], suggesting that hypoperfusion in the frontal cortex in responders likely reflected brain dysfunction responsible for psychiatric symptoms at baseline. The difference in patient profiles between their and our studies may be due to a selection bias in their study, because a small number of patients who underwent SPECT examination were selected from a large group of AD patients [10].

5. Conclusion

In summary, SPECT examinations may be useful in the prediction of behavioral responses to donepezil. Donepezil

treatment may be beneficial in AD patients if the parieto-temporal associative cortices are not severely affected and rCBF in the premotor cortex is preserved.

Acknowledgment

This work was supported by Research Grants for Longevity Sciences (15C-3) and for Comprehensive Research on Aging and Health (H14-choju-012) from the Ministry of Health, Labor, and Welfare of Japan.

References

[1] Cummings JL. Use of cholinesterase inhibitors in clinical practice: evidence-based recommendations. Am J Geriatr Psychiatry 2003; 11(2):131–45.
[2] Doody RS, Geldmacher DS, Gordon B, Perdomo CA, Pratt RD. Open-label, multicenter, phase 3 extension study of the safety and efficacy of donepezil in patients with Alzheimer disease. Arch Neurol 2001;58(3):427–33.
[3] Mohs RC, Doody RS, Morris JC, Ieni JR, Rogers SL, Perdomo CA, et al. A 1-year, placebo-controlled preservation of function survival study of donepezil in AD patients. Neurology 2001;57(3):481–8.
[4] Winblad B, Engedal K, Soininen H, Verhey F, Waldemar G, Wimo A, et al. A 1-year, randomized, placebo-controlled study of donepezil in patients with mild to moderate AD. Neurology 2001;57(3):489–95.
[5] Rogers SL, Farlow MR, Doody RS, Mohs R, Friedhoff LT. A 24-week, double-blind, placebo-controlled trial of donepezil in patients with Alzheimer's disease, Donepezil study group. Neurology 1998; 50(1):136–45.
[6] Nakano S, Asada T, Matsuda H, Uno M, Takasaki M. Donepezil hydrochloride preserves regional cerebral blood flow in patients with Alzheimer's disease. J Nucl Med 2001;42(10):1441–5.
[7] Nobili F, Koulibaly M, Vitali P, Migneco O, Mariani G, Ebmeier K, et al. Brain perfusion follow-up in Alzheimer's patients during treatment with acetylcholinesterase inhibitors. J Nucl Med 2002;43(8):983–90.
[8] Hanyu H, Shimizu T, Tanaka Y, Takasaki M, Koizumi K, Abe K. Regional cerebral blood flow patterns and response to donepezil treatment in patients with Alzheimer's disease. Dement Geriatr Cogn Disord 2003;15(4):177–82.
[9] Mega MS, Masterman DM, O'Connor SM, Barclay TR, Cummings JL. The spectrum of behavioral responses to cholinesterase inhibitor therapy in Alzheimer disease. Arch Neurol 1999;56(11):1388–93.
[10] Mega MS, Dinov ID, Lee L, O'Connor SM, Masterman DM, Wilen B, et al. Orbital and dorsolateral frontal perfusion defect associated with behavioral response to cholinesterase inhibitor therapy in Alzheimer's disease. J Neuropsychiatry Clin Neurosci 2000;12(2): 209–18.
[11] Greene JG, Smith R, Gardiner M, Timbury GC. Measuring behavioural disturbance of elderly demented patients in the community and its effects on relatives: a factor analytic study. Age Ageing 1982;11(2):121–6.
[12] Kaufer DI, Cummings JL, Christine D, Bray T, Castellon S, Masterman D, et al. Assessing the impact of neuropsychiatric symptoms in Alzheimer's disease: the neuropsychiatric inventory caregiver distress scale. J Am Geriatr Soc 1998;46(2):210–5.
[13] Fillit HM, Gutterman EM, Brooks RL. Impact of donepezil on caregiving burden for patients with Alzheimer's disease. Int Psychogeriatr 2000;12(3):389–401.
[14] Landes AM, Sperry SD, Strauss ME, Geldmacher DS. Apathy in Alzheimer's disease. J Am Geriatr Soc 2001;49(12):1700–7.
[15] Feldman H, Gauthier S, Hecker J, Vellas B, Emir B, Mastey V, et al. Efficacy of donepezil on maintenance of activities of daily living in patients with moderate to severe Alzheimer's disease and the effect on caregiver burden. J Am Geriatr Soc 2003;51(6):737–44.
[16] McKhann G, Drachman D, Folstein M, Katzman R, Price D, Stadlan EM. Clinical diagnosis of Alzheimer's disease: report of the NINCDS-ADRDA Work Group under the auspices of Department of Health and Human Services Task Force on Alzheimer's Disease. Neurology 1984;34(7):939–44.
[17] Cummings JL, Mega M, Gray K, Rosenberg-Thompson S, Carusi J, Gornbein J. The Neuropsychiatric Inventory: comprehensive assessment of psychopathology in dementia. Neurology 1994;44(12): 2308–14.
[18] Mahoney F, Barthel D. Functional evaluation; the Barthel index. Md State Med J 1965;14:61–5.
[19] Lawton MP, Brody EM. Assessment of older people: self-maintaining and instrumental activities of daily living. Gerontologist 1969;9(3): 179–86.
[20] Vennerica A, Shanks MF, Staff RT, Pestell SJ, Forbes KE, Gemmell HG, et al. Cerebral blood flow and cognitive responses to rivastigmine treatment in Alzheimer's disease. NeuroReport 2002;13(1):83–7.
[21] Eger E, Sterzer P, Russ MO, Giraud AL, Kleinschmidt A. A supramodal number representation in human intraparietal cortex. Neuron 2003;37(4):719–25.
[22] Grossman M, Koenig P, Glosser G, DeVita C, Moore P, Rhee J, et al. Neural basis for semantic memory difficulty in Alzheimer's disease: an fMRI study. Brain 2003;126(Pt 2):292–311.
[23] Moll J, de Oliveira-Souza R, Bramati IE, Grafman J. Functional networks in emotional moral and nonmoral social judgments. NeuroImage 2002;16(3 Pt 1):696–703.
[24] Verney SP, Brown GG, Frank L, Paulus MP. Error-rate-related caudate and parietal cortex activation during decision making. NeuroReport 2003;14(7):923–8.
[25] Paulesu E, Frith CD, Frackowiak RS. The neural correlates of the verbal component of working memory. Nature 1993;362(6418): 342–5.
[26] Jonides J, Smith EE, Koeppe RA, Awh E, Minoshima S, Mintun MA. Spatial working memory in humans as revealed by PET. Nature 1993;363(6430):623–5.
[27] Schumacher EH, Lauber E, Awh E, Jonides J, Smith EE, Koeppe RA. PET evidence for an amodal verbal working memory system. NeuroImage 1996;3(2):79–88.
[28] Jonides J, Smith EE, Marshuetz C, Koeppe RA, Reuter-Lorenz PA. Inhibition in verbal working memory revealed by brain activation. Proc Natl Acad Sci U S A 1998;95(14):8410–3.
[29] Smith EE, Jonides J. Storage and executive processes in the frontal lobes. Science 1999;283(5408):1657–61.
[30] Reuter-Lorenz PA, Jonides J, Smith EE, Hartley A, Miller A, Marshuetz C, et al. Age differences in the frontal lateralization of verbal and spatial working memory revealed by PET. J Cogn Neurosci 2000;12(1):174–87.
[31] Hanakawa T, Honda M, Sawamoto N, Okada T, Yonekura Y, Fukuyama H, et al. The role of rostral Brodmann area 6 in mental-operation tasks: an integrative neuroimaging approach. Cereb Cortex 2002;12(11):1157–70.
[32] Hopfinger JB, Buonocore MH, Mangun GR. The neural mechanisms of top-down attentional control. Nat Neurosci 2000;3(3):284–91.
[33] Boussaoud D. Attention versus intention in the primate premotor cortex. NeuroImage 2001;14(1 Pt 2):S40–5.
[34] Ohbayashi M, Ohki K, Miyashita Y. Conversion of working memory to motor sequence in the monkey premotor cortex. Science 2003; 301(5630):233–6.

Available online at www.sciencedirect.com
SCIENCE DIRECT®
Biochemical and Biophysical Research Communications 321 (2004) 345–349
BBRC
www.elsevier.com/locate/ybbrc

Activators of PPARγ antagonize protection of cardiac myocytes by endothelin-1

Natsuhiko Ehara [a], Koji Hasegawa [b,*], Koh Ono [b], Teruhisa Kawamura [b], Eri Iwai-Kanai [a], Tatsuya Morimoto [a], Masaharu Akao [a], Souichi Adachi [c], Toru Kita [a]

[a] *Department of Cardiovascular Medicine, Graduate School of Medicine, Kyoto University, 54 Kawara-cho, Shogoin, Sakyo-ku, Kyoto 606-8507, Japan*
[b] *Division of Translational Research, Kyoto Medical Center, National Hospital Organization, 1-1 Mukaihata-cho, Fukakusa, Fushimi-ku, Kyoto 612-8555, Japan*
[c] *Department of Pediatrics, Graduate School of Medicine, Kyoto University, 54 Kawara-cho, Shogoin, Sakyo-ku, Kyoto 606-8507, Japan*

Received 14 May 2004

Abstract

Endothelin-1 (ET-1) is a potent survival factor against myocardial cell apoptosis. This anti-apoptotic effect of ET-1 is mediated in part through calcineurin/NFATc-dependent induction of bcl-2 expression. Since it has been reported that peroxisome proliferator-activated receptor-γ (PPARγ) interacts with NFATc, we investigated the effects of PPARγ ligands on anti-apoptotic effects of ET-1 in cardiac myocytes. In primary cardiac myocytes from neonatal rats, administration of PPARγ activators (15-deoxy-$\Delta^{12,14}$-prostaglandin J_2 and troglitazone) attenuated the anti-apoptotic effects of ET-1. These activators abolished the ET-1-stimulated increase in bcl-2 expression and in binding of cardiac NFATc to the bcl-2 NFAT site. These findings demonstrate that activators of PPARγ perturb the anti-apoptotic effects of ET-1 in cardiac myocytes and that this perturbation is, in part, based on functional transcriptional cross-talk between NFATc and PPARγ.

Keywords: Apoptosis; Bcl-2; Cardiac myocyte; ET-1; NFATc; PPARγ

Accumulating evidence suggests that apoptosis occurs in cardiac myocytes in vivo and contributes to the impairment of cardiac function. A number of humoral factors are activated in congestive heart failure [1], and they may possibly play positive and negative roles in the regulation of cardiac cell apoptosis. Endothelin-1 (ET-1) is one such factor: it acts not only as a vasoconstrictive and growth-promoting peptide, but also as a survival factor against apoptosis [2–4]. Stimulation with ET-1 results in an increase in intracellular calcium levels [5]. The calcium-activated phosphatase calcineurin is necessary for the nuclear import of the nuclear factor of activated T lymphocyte (NFAT) transcription factors, which mediate changes in gene expression in response to calcium signaling from the T-cell receptor [6]. We reported previously that stimulation of cardiac myocytes with ET-1 increases the expression of bcl-2 protein and inhibits oxidant stress-induced apoptosis via the calcineurin–NFATc pathway in cardiac myocytes [7].

The peroxisome proliferator-activated receptors (PPARs) are ligand-activated transcription factors and members of the nuclear hormone receptor superfamily. PPARγ, the most intensively studied isoform, has been implicated in such diverse pathways as lipid and glucose homeostasis, control of cellular proliferation and differentiation [8,9]. It is reported that activated PPARγ physically associates with the transcription factor NFATc and blocks NFATc/DNA binding and transcriptional activity [10,11]. Therefore, we hypothesized that activation of PPARγ might impair the ET-1-dependent calcineurin/NFAT pathway and inhibit the anti-apoptotic

* Corresponding author. Fax: +81-75-641-9252.
E-mail address: koj@kuhp.kyoto-u.ac.jp (K. Hasegawa).

0006-291X/$ - see front matter © 2004 Elsevier Inc. All rights reserved.
doi:10.1016/j.bbrc.2004.06.147

effect of ET-1 in cardiac myocytes. The present study was performed to test this hypothesis.

Materials and methods

TUNEL staining and FITC-linked annexin V/propidium iodide staining. DNA cleavage was detected by the TdT-mediated dUTP nick end labeling (TUNEL) assay in primary ventricular cardiac myocytes prepared from neonatal rats as previously described [4,12]. For the annexin V assay, cells were washed with ice-cold PBS and resuspended in 1× annexin-binding buffer (10 mM Hepes, 140 mM NaCl, and 2.5 mM $CaCl_2$, pH 7.4). Five milliliters of annexin V-fluorescein isothiocyanate and 1 ml of 100 mg/mL propidium iodide working solution were added to 100 ml of cell suspension. The cells were gently mixed and incubated at room temperature for 15 min. Six randomly selected fields were counted using a fluorescent microscope (NIKON Eclipse TE 300). Subsequent image capture and analysis were performed using image analysis software. The number of stained cells was normalized by the total number of cells counted by phase microscopy of the same field.

Western blotting analysis. Western blotting was performed as previously described [13]. For detection of bcl-2, bax, bcl-xL, and β-actin, we used an anti-rat bcl-2 monoclonal antibody (Medical & Biological Laboratories), an anti-rat bax monoclonal antibody (Neo Markers), an anti-rat bcl-x monoclonal antibody (Transduction Laboratories), and an anti-β actin monoclonal antibody (Sigma). The images were analyzed with computer-assisted densitometry (NIH Image software).

Electrophoretic mobility shift assays. Nuclear extracts were prepared from cultures of primary neonatal rat cardiac myocytes as previously described [13–15]. Double-stranded oligonucleotides were designed to contain the NFAT-binding sites in the human bcl-2 promoter. The sequences of the sense strands of these oligonucleotides were as follows: WT, 5′-CCTTTTTAGGAAAAGAGGGAAAAAAT AAAACCC-3′; and MT, 5′-CCTTTTTAGCTCCCGAGGCTCCC AATAAAACCC-3′. Electrophoretic mobility shift assays (EMSAs) were carried out as described previously [13–15]. Protein–DNA complexes were separated by electrophoresis on 4% nondenaturing polyacrylamide gels in 0.25× TBE (1× TBE is 100 mM Tris, 100 mM boric acid, and 2 mM EDTA) at 4 °C. The images were analyzed with computer-assisted densitometry (NIH Image software).

Immunocytochemistry. Cardiac myocytes were grown in flask-style chambers containing glass slides (Nalgen Nunc). Immunocytochemical staining for NFATc was performed by using the indirect immunofluorescence method. The cells were fixed with Bouin's solution for 10 min at room temperature and subsequently autoclaved for 10 min at 121 °C in 10 mM citrate, pH 6.0. The cells were incubated with anti-NFATc monoclonal antibody (Santa Cruz Biotechnology) at a dilution of 1:100. NFATc signals were detected with anti-mouse FITC-conjugated secondary antibody at a dilution of 1:500 for 45 min.

Statistical analysis. Data are presented as means ± SE. Statistical comparisons were performed by using unpaired two-tailed Student's *t* test or ANOVA with Scheffe's test when appropriate, with a probability value less than 0.05 taken to indicate significance.

Results and discussion

Activators of PPARγ (15-deoxy-$\Delta^{12,14}$-prostaglandin J_2 and troglitazone) antagonize the anti-apoptotic effect of ET-1

Since a body of evidence suggests that reactive oxygen species (ROS) are involved in cardiac pathophysiology and can trigger myocyte apoptosis [16,17], we utilized H_2O_2 as an inducer of myocardial cell apoptosis in this study. To examine changes in the anti-apoptotic effect of ET-1 by activators of PPARγ (15-deoxy-$\Delta^{12,14}$-prostaglandin J_2 (15d-PGJ_2) or troglitazone), neonatal rat cardiac myocytes were treated with these reagents in combination with H_2O_2 (10 μM) and/or ET-1 (100 nM) in serum-free medium for 48 h. Under our experimental conditions, the percentage of TUNEL-positive cells was 13% in the saline-stimulated basal state (panel a in Fig. 1A and bar 1 in Fig. 1B).

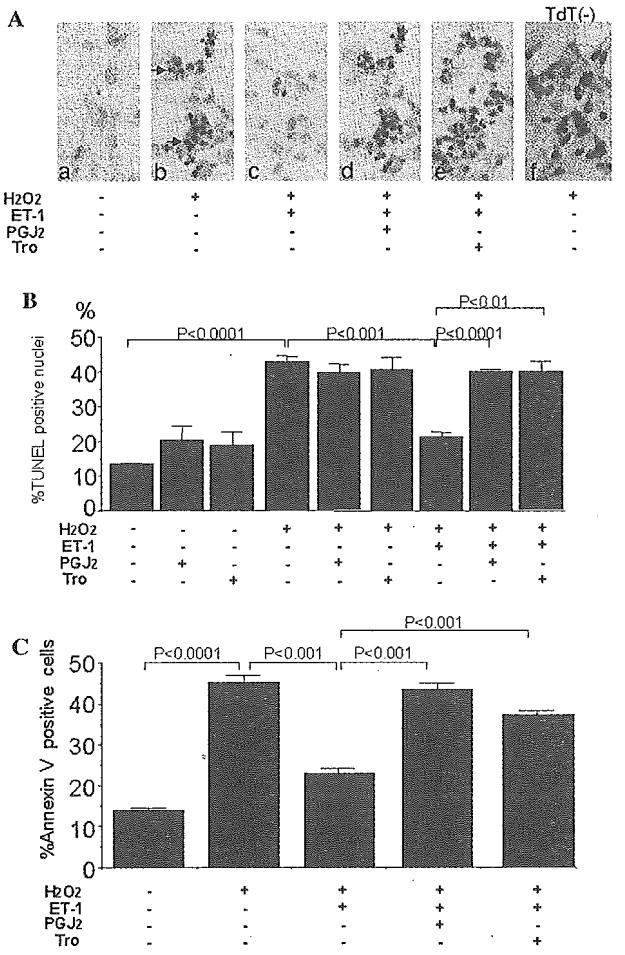

Fig. 1. Activators of PPARγ antagonize protective effect of ET-1 against H_2O_2-induced apoptosis in cardiac myocytes. Neonatal rat cardiac myocytes were cultured in serum-free medium in the presence or absence of H_2O_2 (10^{-5} mol/L), ET-1 (10^{-7} mol/L), 15d-PGJ_2 (2×10^{-6} mol/L) or troglitazone (2×10^{-6} mol/L) for 48 h. (A) Representative photographs of TUNEL-staining. Terminal deoxynucleotidyltransferase (TdT) was omitted in panel f. Arrowheads show cells with characteristics of apoptosis, including chromatin condensation. (B) Quantitative analysis of TUNEL staining. TUNEL-positive nuclei were counted and expressed as the percentage of total nuclei. An average of 400–500 nuclei were counted in random fields on each slide. The results are means ± SE of 3 independent experiments. (C) Quantitative analysis of annexin V staining. The number of stained cells was normalized by the total number of cells counted by phase microscopy of the same field. An average of 400–500 nuclei were counted in random fields on each slide. The results are means ± SE of 3 independent experiments.

Stimulation with 15d-PGJ_2 (2 μM) or troglitazone (2 μM) alone did not significantly increase the number of TUNEL-positive cells (bars 2, 3 in Fig. 1B). However, stimulation with H_2O_2 markedly increased the number of TUNEL-positive cells (panel b in Fig. 1A and bar 4 in Fig. 1B). These TUNEL-positive cells may specifically indicate the presence of internucleosomal DNA fragmentation, because no positive cells were found when we omitted the terminal deoxytransferase treatment (panel f in Fig. 1A). The cells stimulated with H_2O_2 displayed small condensed nuclei, cell shrinkage, and nuclear fragmentation, consistent with the morphological features of apoptosis. Compatible with our previous report, the number of H_2O_2-induced TUNEL-positive cells was decreased by treatment with ET-1 (panel c in Fig. 1A and bar 7 in Fig. 1B). Notably, 15d-PGJ_2 or troglitazone antagonized the anti-apoptotic effect of ET-1 (panels d and e in Fig. 1A, and bars 8 and 9 in Fig. 1B). Stimulation with 15d-PGJ_2 or troglitazone in addition to H_2O_2 did not increase the number of TUNEL-positive cells (bars 5 and 6 in Fig. 1B) compared with stimulation with H_2O_2 alone.

To monitor the translocation of phosphatidylserine from the inner to the outer leaflet of the plasma membrane, we examined cellular binding of annexin V as an index of the early stages of cell apoptosis. As shown in Fig. 1C, the percentage of annexin V-labeled cells was 15% in the basal state (bar 1). Consistent with the data of TUNEL staining, stimulation with H_2O_2 markedly increased the number of annexin V-labeled myocardial cells (bar 2). The number of annexin V-labeled myocardial cells decreased after treatment with ET-1 in addition to H_2O_2 (bar 3). However, 15d-PGJ_2 or troglitazone antagonized the anti-apoptotic effect of ET-1 (bars 4 and 5). Taken together with the data of TUNEL staining, these findings demonstrate that activators of PPARγ, 15d-PGJ_2 and troglitazone, abolished the protective effect of ET-1 against H_2O_2-induced apoptosis.

15d-PGJ_2 and troglitazone inhibit the ET-1-induced increase in cardiac bcl-2 protein levels

To determine whether stimulation of cardiac myocytes with PPARγ ligands decreased the ET-1-induced bcl-2 expression, neonatal cardiac myocytes were treated with ET-1 in the presence or absence of 15d-PGJ_2 (2 μM) or troglitazone (2 μM). Forty-eight hours later, lysates from these cells were subjected to Western blotting with anti-bcl-2 antibody. As shown in Figs. 2A and B, ET-1 stimulation induced the expression of bcl-2 protein by 2.9 ± 0.5-fold (lane 4) compared with saline stimulation (lane 1). Treatment with 15d-PGJ_2 or troglitazone inhibited the induction of bcl-2 expression by ET-1 to almost the control level (lanes 5 and 6). Stimulation with 15d-PGJ_2 or troglitazone alone did not change the expression of bcl-2 protein compared with saline stimulation (lanes 2 and 3). None of these stimuli altered the expression of the pro-apoptotic molecule bax or the anti-apoptotic molecule bcl-xL.

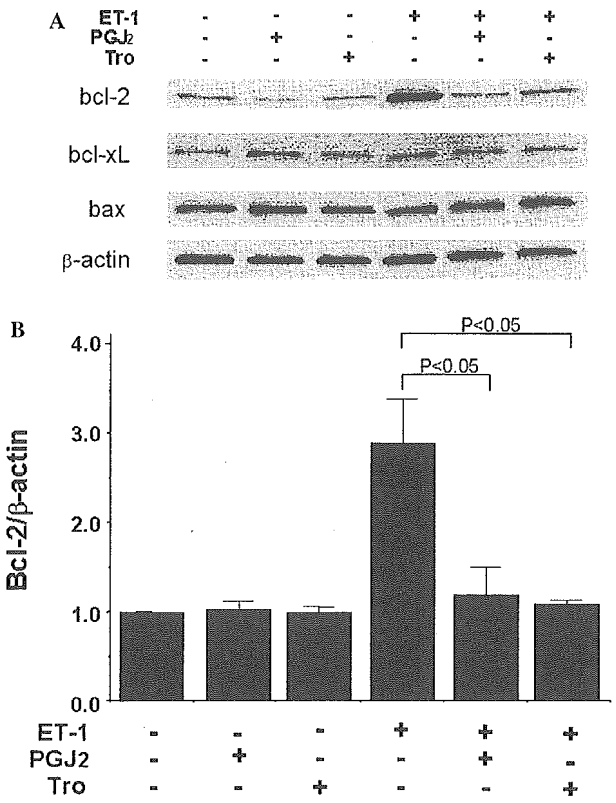

Fig. 2. Activators of PPARγ inhibit ET-1-induced increase of bcl-2 expression. Cardiac myocytes were stimulated with troglitazone (2×10^{-6}mol/L) or 15d-PGJ_2 (2×10^{-6}mol/L) in the presence or the absence of ET-1 (10^{-7}mol/L) for 48 h. Cell lysates were subjected to Western blotting with an anti-bcl-2 antibody, anti-bax antibody, anti-bcl-xL antibody or anti-β-actin antibody. The images were analyzed with computer-assisted densitometry (NIH Image software).

Troglitazone abolishes the ET-1-stimulated increase in the DNA binding of cardiac NFATc

We previously reported that ET-1-induced upregulation of bcl-2 expression is mediated, in part, at the level of transcription and that mutation of NFAT sites within the bcl-2 promoter completely abolished the ET-1-responsiveness of bcl-2 transcription [18]. Therefore, the present study investigated the functional association of PPARγ with NFATc in cardiac myocytes. To examine the nuclear translocation of endogenous NFATc in response to treatment with ET-1 and troglitazone in cardiac myocytes, we performed immunofluorescence microscopic analysis. As shown in Fig. 3A, NFATc was detected in the cytoplasm of nearly all saline-stimulated cardiac myocytes (panel a). However, the stimulation of cardiac myocytes with ET-1 markedly changed this localization and caused the nuclear translocation of NFATc (panel b), indicating activation of the

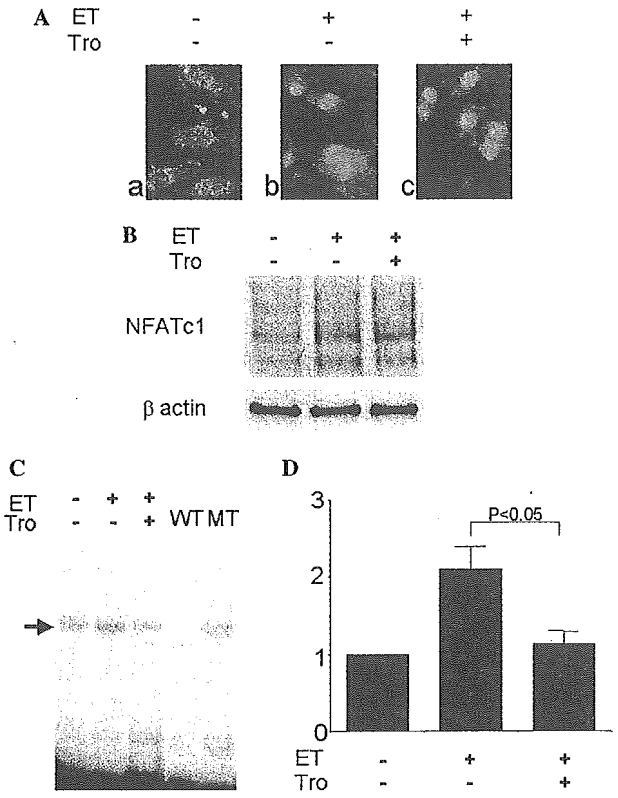

Fig. 3. Troglitazone abolishes the ET-1-stimulated increase in the DNA binding of cardiac NFATc. Cardiac myocytes were treated with ET-1 (10^{-7} mol/L), ET-1 plus troglitazone (2×10^{-6} mol/L), or saline as a control for 48 h in serum-free conditions in culture. (A) Cells were subjected to immunofluorescence with an anti-NFATc antibody. (B) Nuclear cell lysates from the cells were subjected to Western blotting with an anti-NFATc antibody. (C) Nuclear extracts from the cells were probed with a radiolabeled oligonucleotide containing the NFAT-binding site in the bcl-2 promoter. For cold competition experiments, a 100-fold molar excess of unlabeled competitor oligonucleotide was included in the binding reaction mixture: WT, wild-type, NFAT-binding site in the bcl-2 promoter; MT, mutant, NFAT-binding site in the bcl-2 promoter with a mutation. (D) The intensity of the specific bands was quantified with computer-assisted densitometry (NIH Image software).

calcineurin/NFATc pathway. Stimulation of cardiac myocytes with troglitazone did not change the nuclear translocation of NFATc induced by ET-1 (panel c).

Nuclear cell lysates derived from these cells were subjected to Western blotting with the anti-NFATc antibody. As shown in Fig. 3B, the level of expression of NFATc was increased slightly by stimulation with ET-1 (lane 2). However, this increase was not affected by treatment with troglitazone in addition to ET-1 (lane 3).

To determine whether activation of PPARγ abolished the ET-1-stimulated increase in the DNA binding of cardiac NFATc, we performed EMSAs. Neonatal cardiac myocytes were treated with ET-1 in the presence or absence of troglitazone for 48 h and nuclear extracts from these cells were probed with a radiolabeled oligonucleotide containing the NFAT-binding site in the bcl-2 promoter in the presence or absence of competitor DNAs. As shown in Fig. 3C, competition EMSAs revealed that a retarded band represented specific binding, as evidenced by the fact that it was competed out by an excess of unlabeled bcl-2 NFAT element (lane 4), but not by the same amount of an oligonucleotide containing the bcl-2 NFAT element with a mutation (lane 5). As shown in Figs. 3C and D, the amount of the specific complex containing NFATc increased in nuclear extracts from ET-1-stimulated myocytes (lane 2) compared with those from saline-treated cells (lane 1). This increase may be, in part, attributable to the increase in the concentration of NFATc in the nuclear extracts, as ET-1-induced nuclear translocation of NFATc. Notably, the ET-1-stimulated increase in the bcl-2 NFAT binding activity was almost completely blocked by troglitazone (lane 3). These findings demonstrate that activation of PPARγ by troglitazone abolished the ET-1-stimulated increase in the binding of cardiac NFATc to the NFAT site in the bcl-2 promoter. Since troglitazone did not change the nuclear localization or protein level of NFATc, the troglitazone-mediated decrease in the DNA binding activity of NFATc might be related to functional association of NFATc with PPARγ. However, further studies will be required to clarify this issue.

Thiazolidinediones are now widely used as insulin-sensitizing agents in patients with diabetes mellitus. However, because of the fluid retention and increase in plasma volume induced by glitazones [19], these agents are contraindicated in the setting of New York Heart Association class III and IV functional status. The present study demonstrated that activators of PPARγ antagonize the protective effects of ET-1 against apoptosis in cardiac myocytes. Thus, additional care may be required for safe administration of glitazones in diabetic patients with heart failure. On the other hand, it has been reported that ligands for PPARγ inhibit cardiac hypertrophy [20,21]. In addition, a PPARγ-dependent signaling pathway is involved in transcription regulating mitochondrial energy metabolism in the heart [8]. Therefore, further studies will be needed to clarify whether PPARγ activation is beneficial or harmful in heart failure.

Acknowledgments

We thank N. Sowa and S. Nagata for excellent technical assistance.

References

[1] M. Packer, The neurohormonal hypothesis: a theory to explain the mechanism of disease progression in heart failure, J. Am. Coll. Cardiol. 20 (1992) 248–254.

[2] J.R. Wu-Wong, W.J. Chiou, R. Dickinson, T.J. Opgenorth, Endothelin attenuates apoptosis in human smooth muscle cells, Biochem. J. 328 (Pt. 3) (1997) 733–737.
[3] M. Shichiri, J.M. Sedivy, F. Marumo, Y. Hirata, Endothelin-1 is a potent survival factor for c-Myc-dependent apoptosis, Mol. Endocrinol. 12 (1998) 172–180.
[4] M. Araki, K. Hasegawa, E. Iwai-Kanai, M. Fujita, T. Sawamura, T. Kakita, H. Wada, T. Morimoto, S. Sasayama, Endothelin-1 as a protective factor against β-adrenergic agonist-induced apoptosis in cardiac myocytes, J. Am. Coll. Cardiol. 36 (2000) 1411–1418.
[5] R.M. Touyz, J. Fareh, G. Thibault, B. Tolloczko, R. Lariviere, E.L. Schiffrin, Modulation of Ca2+ transients in neonatal and adult rat cardiomyocytes by angiotensin II and endothelin-1, Am. J. Physiol. 270 (1996) H857–868.
[6] A. Rao, C. Luo, P.G. Hogan, Transcription factors of the NFAT family: regulation and function, Annu. Rev. Immunol. 15 (1997) 707–747.
[7] T. Kakita, K. Hasegawa, E. Iwai-Kanai, S. Adachi, T. Morimoto, H. Wada, T. Kawamura, T. Yanazume, S. Sasayama, Calcineurin pathway is required for endothelin-1-mediated protection against oxidant stress-induced apoptosis in cardiac myocytes, Circ. Res. 88 (2001) 1239–1246.
[8] D. Bishop-Bailey, Peroxisome proliferator-activated receptors in the cardiovascular system, Br. J. Pharmacol. 129 (2000) 823–834.
[9] E.D. Rosen, B.M. Spiegelman, PPARgamma: a nuclear regulator of metabolism, differentiation, and cell growth, J. Biol. Chem. 276 (2001) 37731–37734.
[10] X.Y. Yang, L.H. Wang, T. Chen, D.R. Hodge, J.H. Resau, L. DaSilva, W.L. Farrar, Activation of human T lymphocytes is inhibited by peroxisome proliferator-activated receptor γ (PPARγ) agonists. PPARγ co-association with transcription factor NFAT, J. Biol. Chem. 275 (2000) 4541–4544.
[11] R.B. Clark, D. Bishop-Bailey, T. Estrada-Hernandez, T. Hla, L. Puddington, S.J. Padula, The nuclear receptor PPARγ and immunoregulation: PPARγ mediates inhibition of helper T cell responses, J. Immunol. 164 (2000) 1364–1371.
[12] E. Iwai-Kanai, K. Hasegawa, M. Araki, T. Kakita, T. Morimoto, S. Sasayama, α- and β-adrenergic pathways differentially regulate cell type-specific apoptosis in rat cardiac myocytes, Circulation 100 (1999) 305–311.
[13] T. Kakita, K. Hasegawa, T. Morimoto, S. Kaburagi, H. Wada, S. Sasayama, p300 protein as a coactivator of GATA-5 in the transcription of cardiac-restricted atrial natriuretic factor gene, J. Biol. Chem. 274 (1999) 34096–34102.
[14] T. Morimoto, K. Hasegawa, S. Kaburagi, T. Kakita, H. Masutani, R.N. Kitsis, A. Matsumori, S. Sasayama, GATA-5 is involved in leukemia inhibitory factor-responsive transcription of the β-myosin heavy chain gene in cardiac myocytes, J. Biol. Chem. 274 (1999) 12811–12818.
[15] T. Morimoto, K. Hasegawa, S. Kaburagi, T. Kakita, H. Wada, T. Yanazume, S. Sasayama, Phosphorylation of GATA-4 is involved in α1-adrenergic agonist-responsive transcription of the endothelin-1 gene in cardiac myocytes, J. Biol. Chem. 275 (2000) 13721–13726.
[16] R. Aikawa, I. Komuro, T. Yamazaki, Y. Zou, S. Kudoh, M. Tanaka, I. Shiojima, Y. Hiroi, Y. Yazaki, Oxidative stress activates extracellular signal-regulated kinases through Src and Ras in cultured cardiac myocytes of neonatal rats, J. Clin. Invest 100 (1997) 1813–1821.
[17] D. Kumar, B.I. Jugdutt, Apoptosis and oxidants in the heart, J. Lab. Clin. Med. 142 (2003) 288–297.
[18] T. Kawamura, K. Ono, T. Morimoto, M. Akao, E. Iwai-Kanai, H. Wada, N. Sowa, T. Kita, K. Hasegawa, Endothelin-1-dependent NFATc signaling associates with transcriptional coactivator p300 in the activation of the bcl-2 promoter in cardiac myocytes, Circ. Res. 94 (2004) 1492–1499.
[19] S. Mudaliar, R.R. Henry, New oral therapies for type 2 diabetes mellitus: The glitazones or insulin sensitizers, Annu. Rev. Med. 52 (2001) 239–257.
[20] K. Yamamoto, R. Ohki, R.T. Lee, U. Ikeda, K. Shimada, Peroxisome proliferator-activated receptor γ activators inhibit cardiac hypertrophy in cardiac myocytes, Circulation 104 (2001) 1670–1675.
[21] M. Asakawa, H. Takano, T. Nagai, H. Uozumi, H. Hasegawa, N. Kubota, T. Saito, Y. Masuda, T. Kadowaki, I. Komuro, Peroxisome proliferator-activated receptor γ plays a critical role in inhibition of cardiac hypertrophy in vitro and in vivo, Circulation 105 (2002) 1240–1246.

ELSEVIER

Atherosclerosis 176 (2004) 289–296

ATHEROSCLEROSIS

www.elsevier.com/locate/atherosclerosis

Heparin-binding EGF-like growth factor induces expression of lectin-like oxidized LDL receptor-1 in vascular smooth muscle cells

Eri Mukai[a,b], Noriaki Kume[a,*], Kazutaka Hayashida[a], Manabu Minami[a], Yuichiro Yamada[b], Yutaka Seino[b], Toru Kita[a]

[a] *Department of Cardiovascular Medicine, Graduate School of Medicine, Kyoto University, 54 Kawahara-cho, Shogoin, Sakyo-ku, Kyoto 606-8507, Japan*
[b] *Department of Diabetes and Clinical Nutrition, Graduate School of Medicine, Kyoto University, 54 Kawahara-cho, Shogoin, Sakyo-ku, Kyoto 606-8507, Japan*

Received 1 May 2003; received in revised form 23 October 2003; accepted 30 March 2004

Available online 23 July 2004

Abstract

Receptor-mediated endocytosis of oxidized LDL (Ox-LDL) has been implicated in lipid accumulation and vascular cell dysfunction. Lectin-like Ox-LDL receptor-1 (LOX-1) is highly inducible by proinflammatory cytokines, as well as angiotensin II and Ox-LDL in vitro. LOX-1 is expressed in macrophages and smooth muscle cells accumulated in the intima of advanced atherosclerotic plaques in vivo. Here we show that heparin-binding epidermal growth factor-like growth factor (HB-EGF), a potent mitogen for vascular smooth muscle cells, induces LOX-1 expression in cultured bovine aortic smooth muscle cells. HB-EGF (1–100 ng/ml) induced LOX-1 expression, which was peaked between 8 and 16 h after HB-EGF stimulation. HB-EGF-induced expression of LOX-1 was suppressed by ZD1839, an inhibitor of EGF receptor phosphorylation. Both MEK and p38 mitogen-activated protein kinase (MAPK) inhibitors significantly blocked LOX-1 upregulation induced by HB-EGF. Phosphatidylinositol 3-kinase (PI3K) inhibitors also blocked HB-EGF-induced LOX-1 expression. HB-EGF induced phosphorylation of ERK, p38 MAPK and Akt, which were suppressed by ZD1839. Upregulated expression of LOX-1 was associated with enhanced uptake of DiI-labeled Ox-LDL in smooth muscle cells. Taken together, HB-EGF can also act as an inducer of LOX-1 expression and play an integral role in foam cell transformation, cellular dysfunction, and proliferation of smooth muscle cells in atherogenesis.

Keywords: Oxidized LDL; Scavenger receptors; LOX-1; HB-EGF; Vascular smooth muscle cells

1. Introduction

Several lines of evidence have suggested that oxidized LDL (Ox-LDL) appears to play key roles in atherogenesis [1,2]. Receptor-mediated binding and uptake of Ox-LDL may be crucial in activation of vascular cells, as well as lipid accumulation and subsequent foam cell transformation [3].

Several different classes of receptors for atherogenic Ox-LDL have been identified and characterized. Among them, lectin-like Ox-LDL receptor-1 (LOX-1) is a 40–50 kDa type II membrane protein with a C-type lectin-like extracellular domain and a short cytoplasmic tail, which was originally cloned in vascular endothelial cells [4]. LOX-1 can support binding, internalization, and degradation of Ox-LDL [5]. Subsequent studies have revealed that expression of LOX-1 can also be found in macrophages [6,7] and activated vascular smooth muscle cells [8–11] in culture. LOX-1 expression is not constitutive, but dynamically induced by proinflammatory cytokines, such as tumor necrosis factor (TNF) α [12] and transforming growth factor (TGF) β [13], angiotensin II [14,15], Ox-LDL [16,17], fluid shear stress [18] at the level of gene transcription. More importantly, LOX-1 is highly expressed by macrophages and smooth muscle cells accumulated in the intima of advanced atherosclerotic lesions, as well as endothelial cells covering early atherosclerotic lesions in vivo [19,20]. These data suggest that LOX-1 may play important roles in both endothelial activation and foam cell transformation of macrophages and vascular smooth muscle cells in atherogenesis.

Heparin-binding epidermal growth factor (EGF)-like growth factor (HB-EGF) is a potent mitogen for vascular smooth muscle cells, which can be expressed by

* Corresponding author. Tel.: +81-75-751-3623; fax: +81-75-751-4094.
E-mail address: nkume@kuhp.kyoto-u.ac.jp (N. Kume).

0021-9150/$ – see front matter © 2004 Elsevier Ireland Ltd. All rights reserved.
doi:10.1016/j.atherosclerosis.2004.03.028

macrophages, endothelial cells, as well as vascular smooth muscle cells [21–23]. HB-EGF can induce migration, proliferation, and phenotypic modulation of smooth muscle cells through its interaction with the EGF receptor [21,23]. Expression of HB-EGF can be induced by proinflammatory cytokines [24], angiotensin II [22], a phospholipid component of Ox-LDL [25–27], as well as fluid shear stress [28]. Furthermore, upregulated expression of HB-EGF in atherosclerotic lesions has also been demonstrated [29–31].

In the present study, therefore, we have tested the hypothesis if HB-EGF may induce expression of LOX-1 in vascular smooth muscle cells.

2. Materials and methods

2.1. Materials

HB-EGF was purchased from R&D Systems. PD98059, SB203580, U0126, LY294002, and wortmannin were from Calbiochem. ZD1839 was a generous gift from AstraZeneca. A mouse anti-bovine LOX-1 monoclonal antibody was prepared by immunization with an recombinant bovine LOX-1 extracelluler domain as previously described [4]. A rat anti-human LOX-1 monoclonal antibody that cross-reacts with bovine LOX-1 was prepared by immunization with an recombinant human LOX-1 extracelluler domain generated by BAC TO BAC Baculovirus Expression System (Life Technologies). Antibodies for ERK and phosphorylated ERK were purchased from Cell Signaling, and antibodies for p38 mitogen-activated protein kinase (MAPK), phosphorylated p38 MAPK, Akt and phosphorylated Akt were from Santa Cruz Biotechnology. Irrelevant rat IgG was purchased from Chemicon.

2.2. Cell culture

Bovine aortic smooth muscle cells (BSMCs) were isolated by an explant method, after removing endothelial cells by scraping the inner surface of bovine aortas with a razor blade, and cultured in DMEM containing 10% (v/v) FBS. Cells were used for experiments at the passage levels between 2 and 6.

2.3. Immunoblot analysis

Cells were washed with phosphate-buffered saline (PBS) and lysed in PBS containing 1% Triton X-100. After heated at 95 °C for 5 min, equal protein concentrations of the cell lysates were subjected to SDS–polyacrylamide (12%) gel electrophoresis and transferred onto nitrocellulose membranes (PROTRAN, Schleicher & Schuell) by electroblotting. After preincubation with blocking buffer (PBS containing 0.1% Tween 20 and 5% nonfat dry milk) for 2 h at room temperature, blotted membranes were incubated with each primary antibody overnight at 4 °C, followed by washing twice with blocking buffer. Membranes were then incubated with a horseradish peroxidase-linked anti-mouse or anti-rabbit IgG (Amersham) for 1 h at room temperature, washed twice in PBS containing 0.04% Tween 20, and visualized by ECL Western blotting detection reagents (Amersham).

2.4. Northern blot analysis

Total cellular RNA was isolated by TRIZOL Reagent (Invitrogen). Total RNA (15 μg) was subjected to electrophoresis through 1% agarose gel containing formaldehyde, and transferred onto nitrocellulose membranes (OPTI-TRAN, Schleicher & Schuell). Membranes were hybridized with a *Xho*I fragment of bovine LOX-1 cDNA which had been labeled with [α-^{32}P] dCTP (Amersham) using random nonamer primers (Megaprime DNA labelling systems, Amersham).

2.5. Cellular uptake of DiI-labeled Ox-LDL

LDL (density: 1.019–1.063 g/ml) was isolated by sequential ultracentrifugation from human plasma. Oxidative modification of LDL was carried out with cupric ion in vitro. Oxidation was monitored by measuring the amount of thiobarbituric acid-reactive substances and electrophoretic mobility of the LDL particles. Our Ox-LDL contained approximately 10 nmol malondialdehyde equivalent/mg protein. Agarose gel electrophoresis showed increased electrophoretic mobility, which is almost equal to that of acetylated LDL, and minimal aggregation of the Ox-LDL particles. Labeling of Ox-LDL with 1,1′-dioctadecyl-3,3,3′,3′-tetramethylindocarbocyanine perchlorate (DiI, Molecular Probes) was performed as previously described [32]. To examine cellular uptake of Ox-LDL, confluent monolayers of BSMCs were incubated with DiI-labeled Ox-LDL (5 μg/ml) in DMEM/10% FBS for additional 2 h after treatment with the indicated reagents for 12 h and washed three times with the cell culture medium. Fluorescence microscopy was performed to detect DiI-Ox-LDL accumulated in cytoplasm.

2.6. Statistical analysis

Data are expressed as the mean ± standard deviations (S.D.). Statistical significance of the differences was evaluated by one-factorial ANOVA followed by Fisher's PLSD test, and $P < 0.05$ was considered significant.

3. Results

3.1. LOX-1 expression is upregulated by HB-EGF in cultured BSMCs

After BSMCs were treated with or without HB-EGF (0.01–100 ng/ml) for 16 h, total cell lysates were isolated

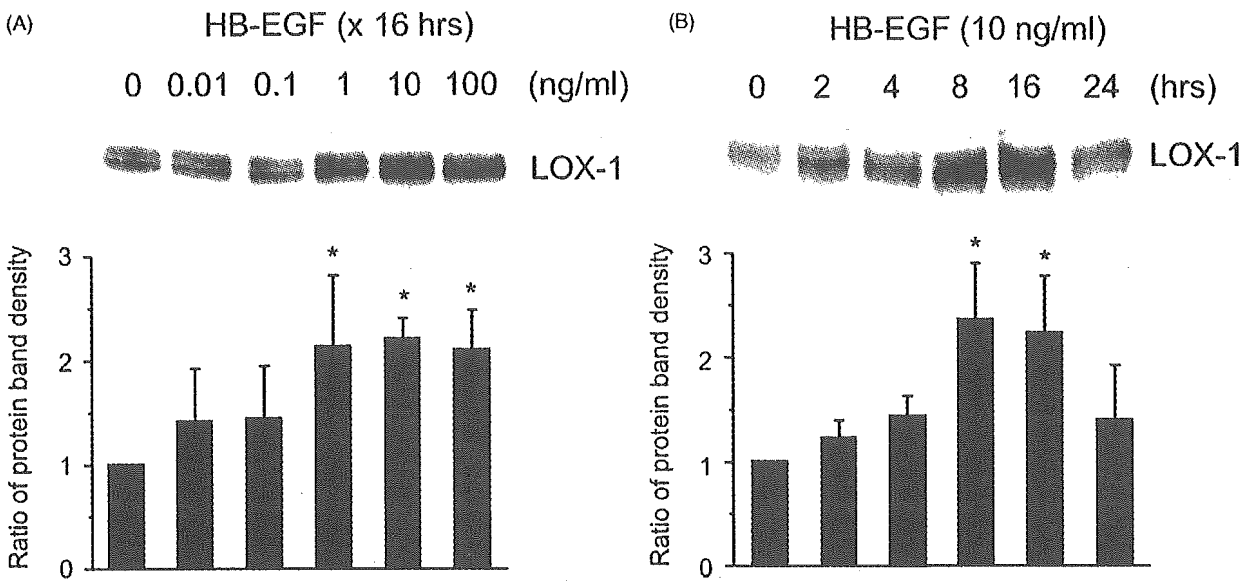

Fig. 1. Effects of HB-EGF on LOX-1 protein induction in BSMCs. After BSMCs were treated with the indicated concentrations of HB-EGF for 16 h (A), or with 10 ng/ml of the reagent for the indicated time periods (B), total cell lysates were subjected to immunoblot analyses with a mouse anti-LOX-1 monoclonal antibody. Data illustrated on the graph bar are the mean ± S.D. of four independent experiments, respectively. $^{*}P < 0.005$ vs. 0 ng/ml of HB-EGF.

and subjected to immunoblot analyses. Fig. 1A demonstrates that LOX-1 protein levels were remarkably induced by HB-EGF in a concentration-dependent manner. Up-regulation of LOX-1 protein expression was observed at concentrations above 1 ng/ml of HB-EGF and peaked at 10 ng/ml of the regent, which resulted in 2.2-fold increase by densitometric analyses. LOX-1 protein expression was time-dependently induced by 10 ng/ml of HB-EGF; increased LOX-1 protein expression was detectable as early as 2 h after the addition of HB-EGF, peaked at 8–16 h (2.4- and 2.3-fold increases, respectively), and declined after 24 h (Fig. 1B).

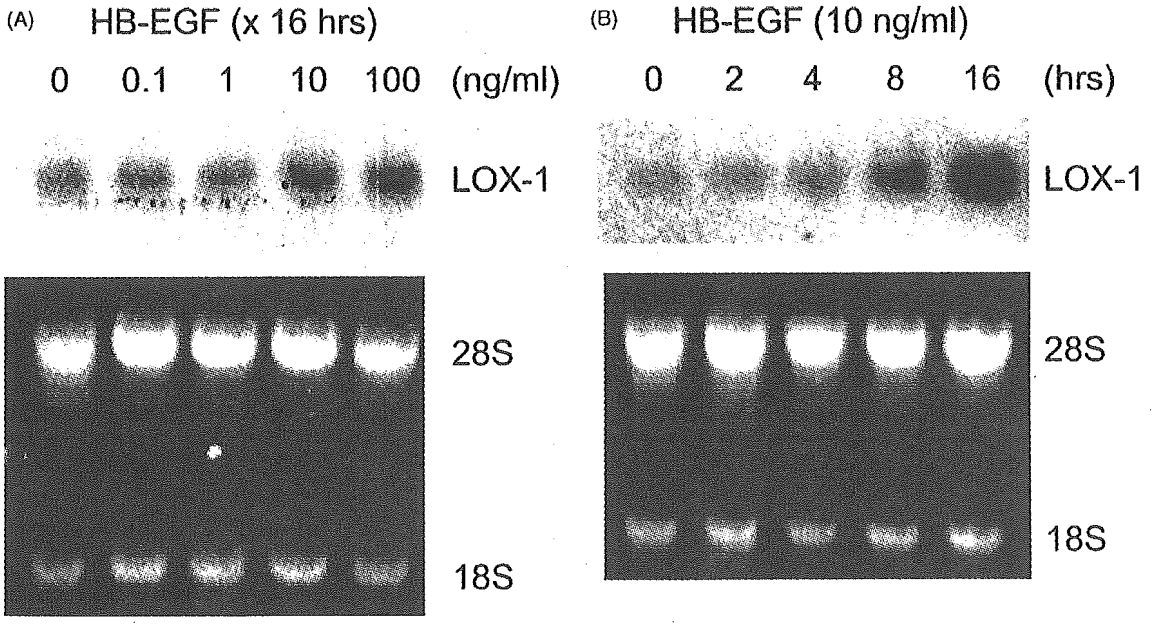

Fig. 2. Effects of HB-EGF on LOX-1 mRNA expression in BSMCs. After BSMCs were treated with the indicated concentrations of HB-EGF for 16 h (A), or with 10 ng/ml of the reagent for the indicated time periods (B), total cellular RNA was subjected to Northern blot analyses (15 μg RNA per lane) with ^{32}P-labeled cDNA probes. Bands for 28S and 18S ribosomal RNA visualized by ethidium bromide staining to control the amount of RNA loaded are also shown.